

A Robust Numerical Path Tracking Algorithm for Polynomial Homotopy Continuation

Simon Telen*

Marc Van Barel†

Jan Verschelde‡

September 11, 2020

Abstract

We propose a new algorithm for numerical path tracking in polynomial homotopy continuation. The algorithm is ‘robust’ in the sense that it is designed to prevent path jumping and in many cases, it can be used in (only) double precision arithmetic. It is based on an adaptive stepsize predictor that uses Padé techniques to detect local difficulties for function approximation and danger for path jumping. We show the potential of the new path tracking algorithm through several numerical examples and compare with existing implementations.

1 Introduction

Homotopy continuation is an important tool in numerical algebraic geometry. It is used for, among others, isolated polynomial root finding and for the numerical decomposition of algebraic varieties into irreducible components. For introductory texts on numerical algebraic geometry and homotopy continuation, we refer to [1, 35, 46, 47, 48] and references therein. The reader who is unfamiliar with algebraic varieties may also consult, e.g., [15] for an excellent introduction.

Let X be an affine variety of dimension n with coordinate ring $R = \mathbb{C}[X]$ (this is the ring of polynomial functions on X , see [15, Chapter 5, §4]) and let $h_i, i = 1, \dots, n$ be elements of $R[t] = \mathbb{C}[X \times \mathbb{C}] = \mathbb{C}[X] \otimes_{\mathbb{C}} \mathbb{C}[t]$. The h_i define the map

$$H : X \times \mathbb{C} \rightarrow \mathbb{C}^n$$

given by $H(x, t) = (h_i(x, t))_{i=1}^n$. Such a map H should be thought of as a family of morphisms $X \rightarrow \mathbb{C}^n$ parametrized by t , which defines a *homotopy* with continuation parameter t . This gives the *solution variety*

$$Z = H^{-1}(0) = \{(x, t) \in X \times \mathbb{C} \mid h_i(x, t) = 0, i = 1, \dots, n\} \subset X \times \mathbb{C}.$$

We will limit ourselves to the cases $X = \mathbb{C}^n, R = \mathbb{C}[x_1, \dots, x_n]$ and $X = (\mathbb{C} \setminus \{0\})^n, R = \mathbb{C}[x_1^{\pm 1}, \dots, x_n^{\pm 1}]$. We will refer to the second case as the *toric case* and $(\mathbb{C} \setminus \{0\})^n$ is called the *algebraic torus*. In both cases, we will use the coordinates $x = (x_1, \dots, x_n)$ on X . Note that for every fixed parameter value $t^* \in \mathbb{C}$, $H_{t^*} : X \rightarrow \mathbb{C}^n : x \mapsto H(x, t^*)$ represents a system of n (Laurent) polynomial equations in n variables with solutions $H_{t^*}^{-1}(0) \subset X$. Typically, for some parameter value $t_0 \in \mathbb{C}$, H_{t_0} is a *start system* with known, isolated and regular solutions and for some other $t_1 \neq t_0$, H_{t_1} represents a *target*

*simon.telen@kuleuven.be

†marc.vanbarel@kuleuven.be, supported by the Research Council KU Leuven, C1-project (Numerical Linear Algebra and Polynomial Computations), and by the Fund for Scientific Research–Flanders (Belgium), G.0828.14N (Multivariate polynomial and rational interpolation and approximation), and EOS Project no 30468160.

‡janv@uic.edu, supported by the National Science Foundation under grant DMS 1854513.

system we are interested in. Consider a point $(z_0, t_0) \in Z$. The task of a homotopy continuation algorithm is to track the point $(z_0, t_0) \in Z$ to a point $(z_1, t_1) \in Z$ along a continuous path

$$\{(x(s), \Gamma(s)), s \in [0, 1]\} \subset Z$$

with $\Gamma : [0, 1] \rightarrow \mathbb{C}$ and $x(s) \in X, s \in [0, 1]$ such that $\Gamma(0) = t_0, x(0) = z_0, \Gamma(1) = t_1, x(1) = z_1$. We will mainly restrict ourselves to paths of the form $\{(x(t), t), t \in [0, 1]\}$ (i.e. $\Gamma(s) = s$), but other Γ will be useful for constructing illustrative examples. The reason for excluding the point $s = 1$ from some of the intervals in these definitions is that continuous paths in Z might ‘escape’ from $X \times \mathbb{C}$ when the parameter t approaches the target value t_1 . For example, solutions may move to infinity or out of the algebraic torus. This kind of behaviour, together with singular points on the path (e.g. *path crossing*) may cause trouble for numerical path tracking (we will make this more precise in Section 2). Many tools have been developed for dealing with such situations [28, 40, 41, 44]. In this paper, we do not focus on this kind of difficulties. Existing techniques can be incorporated in the algorithms we present.

In typical constructions, such as linear homotopies for polynomial system solving, H is randomized such that the paths that need to be tracked do not contain singular points with probability one [48]. This implies for example that all paths are disjoint. However, there might be singularities very near the path in the parameter space. In this situation, the coordinates in X along the path may become very large, which causes scaling problems¹, or two different paths may be very near to each other for some parameter values. The latter phenomenon causes *path jumping*, which is considered one of the main problems for numerical path trackers. Path jumping occurs when along the way, the solution that’s being tracked ‘jumps’ from one path to another. The typical reason is that starting from a point in $H_{t^*}^{-1}(0)$, the *predictor* step in the path tracking algorithm returns a point in $X \times \{t^* + \Delta t\}$ which, according to the *corrector* step, is a numerical approximation of a point in $H_{t^* + \Delta t}^{-1}(0)$ which is on a different path than the one being tracked. It is clear that path jumping is more likely to occur in the case where two or more paths come near each other. Ideally, a numerical path tracker should take small steps Δt in such ‘difficult’ regions and larger steps where there’s no risk for path jumping. There have been many efforts to design such *adaptive stepsize* path trackers [22, 33, 45, 53]. However, the state of the art homotopy software packages such as PHCpack [60], Bertini [5] and HomotopyContinuation.jl [11] still suffer from path jumping, as we will show in our experiments. A typical way to adjust the stepsize is by an *a posteriori* step control. This is represented schematically (in a simplified way) by Figure 1. In the figure, $0 < \beta < 1$ is a real constant, the $\|\cdot\|$ should be

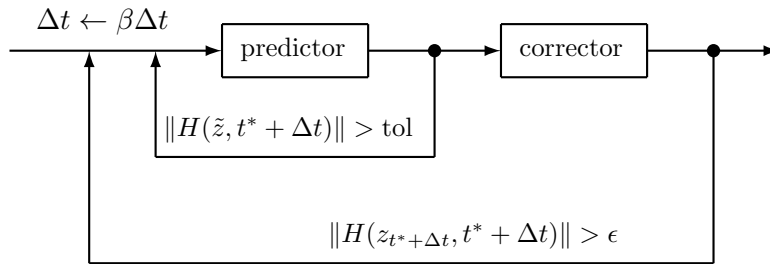


Figure 1: Two feedback loops in a predictor-corrector method for a posteriori step control.

interpreted as a relative measure of the backward error and \tilde{z} is the predicted solution which is refined to $z_{t^* + \Delta t}$ by the corrector. If $\text{tol} \leq \epsilon$, then the corrector stage is not needed. If $\text{tol} = \infty$, then the

¹Scaling problems caused by large coordinates can be resolved in homogeneous coordinates, after a projective transformation [39].

first feedback loop never happens. Such extreme choices for tol are not recommended. With well chosen values for tol and ϵ , the second feedback loop never occurs, as Newton’s method converges to the required accuracy of ϵ in just a couple of steps. This type of feedback loops is implemented in, e.g., PHCpack [60] and Bertini [4]. Recently, Sascha Timme has developed a new adaptive stepsize algorithm that is implemented in HomotopyContinuation.jl (v1.1) [53]. In this algorithm, the first Δt that enters the loop in Figure 1 is computed such that it is an (estimate for an) upper bound for all ‘feasible stepsizes’, and the corrected stepsize in case of rejection is computed in a novel way. For details, see [53].

Certified path trackers have been developed to prevent path jumping [8, 13, 58, 64], but they require more computational effort. Moreover, the certification assumes that the coefficients of the input systems are exact rational numbers, as stated in [8].

In this paper, we propose an adaptive stepsize path tracking algorithm that is robust yet efficient. As opposed to standard methods, we use *a priori* step control: we compute the appropriate stepsize *before* taking the step. We use Padé approximants [3] of the solution curve $x(t)$ in the predictor step, not only to generate a next approximate solution, but also to detect nearby singularities in the parameter space. In the case of type $(L, 1)$ approximants (see Section 3 for a definition), this is a direct application of Fabry’s ratio theorem (Theorem 3.4). The Padé approximants are computed from the series expansion of $x(t)$. We use the iterative, symbolic-numeric algorithm from [10] to compute this series expansion. For an appropriate starting value $x^{(0)}(t) \in \mathbb{C}[[t]]$, we prove ‘second order convergence’ of this iteration in the sense that $x(t) - x^{(k)}(t) = 0 \pmod{\langle t^{2k} \rangle}$ where $x^{(k)}(t) \in \mathbb{C}[[t]]$ is the approximate series solution after the k -th iteration and $\langle \cdot \rangle$ denotes the ideal generated in the power series ring $\mathbb{C}[[t]]$ (see Proposition 4.2). We use information contained in the Padé approximant to determine a trust region for the predictor and use this as a first criterion to compute the adaptive stepsize. A second criterion is based on an estimate for the distance to the most nearby path and a standard approximation error estimate for the Padé approximant.

We note that Padé approximants have been used before in path tracking algorithms [22, 45]. In these articles, their use has been limited to type $(2, 1)$ Padé approximants (see later for a definition) and they have not been used as nearby singularity detectors. In [30], Padé approximants are used in the context of symbolic deformation methods. Padé approximants are applied to solve nonlinear systems arising in power systems [56]. In [57], conceptual differences with continuation methods are discussed. Recent practical comparisons between this holomorphic embedding based continuation method and polynomial homotopy continuation can be found in [63].

The paper is organized as follows. In the next section, we describe numerical path tracking algorithms for smooth paths in general and give some examples. In Section 3 we discuss fractional power series solutions and Padé approximants. Section 4 contains a description of an algorithm introduced in [10] to compute power series solutions and a new proof of convergence. The resulting path tracking algorithm is described in Section 5 and implemented in version 2.4.72 of PHCpack, which is available on github. We show the algorithm’s effectiveness through several numerical experiments in Section 6. We compare with the built-in path tracking routines in (previous versions of) PHCpack [60], Bertini [5] and HomotopyContinuation.jl [11].

2 Tracking Smooth Paths

Let $H(x, t) : X \times \mathbb{C} \rightarrow \mathbb{C}^n$ be as in the introduction where X is either \mathbb{C}^n or $(\mathbb{C} \setminus \{0\})^n$. We denote $Z = H^{-1}(0)$ and we assume that $\dim(Z) = 1$. To avoid ambiguities, we will denote t for the coordinate on \mathbb{C} in $X \times \mathbb{C}$ and $t^* \in \mathbb{C}$ for points in \mathbb{C} . We define the projection map $\pi : Z \rightarrow \mathbb{C} : (x, t) \mapsto t$. By [48, Theorem 7.1.1] π is a ramified cover of \mathbb{C} with ramification locus S consisting of a finite set of points in \mathbb{C} , such that the fiber $\pi^{-1}(t^*)$ consists of a fixed number $\deg \pi = \delta \in \mathbb{N}$ of points in Z if and

only if $t^* \in \mathbb{C} \setminus S$. Let

$$J_H(x, t) = \left(\frac{\partial h_i}{\partial x_j} \right)_{i,j=1,\dots,n}$$

be the Jacobian matrix of H with respect to the x_j .

Definition 2.1. Let H, Z be defined as above. Let $\Gamma : [0, 1] \rightarrow \mathbb{C}$ and let $P = \{(x(s), \Gamma(s)), s \in [0, 1]\} \subset Z$ be a continuous path in Z . We say that P is smooth if $J_H(x, t) \in \text{GL}(n, \mathbb{C})$ for all $(x, t) \in P$.

If $P = \{(x(s), \Gamma(s)) \mid s \in [0, 1]\} \subset Z$ is continuous with $\Gamma([0, 1]) \cap S = \emptyset$, then $P \subset \pi^{-1}(\mathbb{C} \setminus S)$ is smooth. In this case, Γ is called a *smooth parameter path*. In more down to earth terms, Γ is smooth if $\{\Gamma(s), s \in [0, 1]\} \subset \mathbb{C}$ contains only parameter values t^* for which H_{t^*} represents a (Laurent) polynomial system with the expected number of regular solutions.

Example 1. Consider the homotopy taken from [33] defined by

$$H(x, t) = x^2 - (t - 1/2)^2 - p^2 \quad (1)$$

where $p \in \mathbb{R}$ is a parameter which we take to be 0.1 in this example. It is clear that a generic fiber $\pi^{-1}(t^*)$ consists of the two points

$$\pm \sqrt{(t^* - 1/2)^2 + p^2}$$

and the ramification locus is $S = \{1/2 \pm p\sqrt{-1}\}$. Note that $J_H = \frac{\partial H}{\partial x}$ is equal to zero at $\pi^{-1}(t^*)$ for $t^* \in S$. We consider three different parameter paths:

$$\begin{aligned} \Gamma_1 : s &\mapsto s, \\ \Gamma_2 : s &\mapsto s - 4ps(s-1)\sqrt{-1}, \\ \Gamma_3 : s &\mapsto s + 0.2\sin(\pi s)\sqrt{-1}. \end{aligned}$$

In Figure 2 these paths are drawn in the complex plane. The background colour at $t^* \in \mathbb{C}$ in this figure corresponds to the absolute value of J_H evaluated at a point in $\pi^{-1}(t^*)$: dark (blue) regions correspond to a small value, as opposed to light (yellow) regions. For each Γ_i , we track two different paths in Z

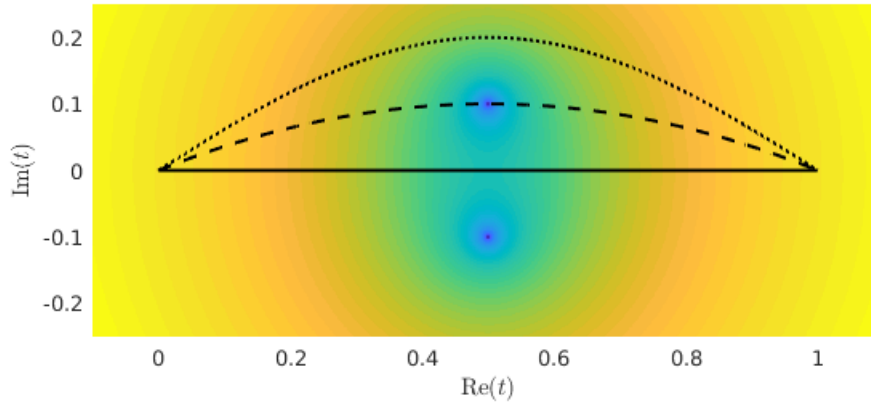


Figure 2: The image of $[0, 1]$ under Γ_1 (full line), Γ_2 (dashed line) and Γ_3 (dotted line) as defined in Example 1.

for $s \in [0, 1]$ starting at $(z_0^{(1)}, 0) = (\sqrt{1/4 + p^2}, 0)$ and $(z_0^{(2)}, 0) = (-\sqrt{1/4 + p^2}, 0)$ respectively. The result is shown in Figure 3. Denote the corresponding paths on Z by $P_j^{(i)} = \{(x^{(i)}(s), \Gamma_j(s)), s \in [0, 1]\}$

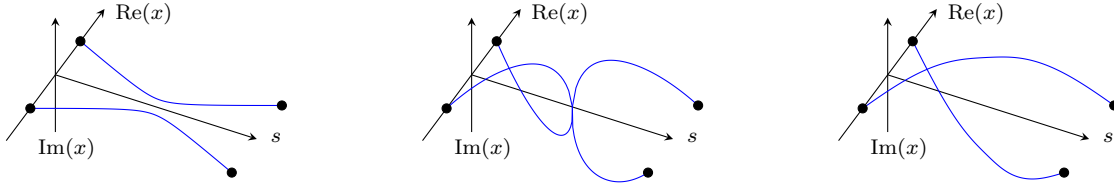


Figure 3: Solution curves with respect to s using, from left to right, Γ_1, Γ_2 and Γ_3 .

where $x^{(i)}(0) = z_0^{(i)}$. Since Γ_1 and Γ_3 do not hit any singular points in the parameter space (Figure 2), the corresponding paths $P_j^{(i)}$ are disjoint and smooth. The paths corresponding to Γ_2 , on the other hand, cross a singularity. They intersect at $s = 1/2$, as can be seen from Figure 3. We conclude that Γ_2 is not smooth. \triangle

An important application of smooth path tracking is the solution of systems of polynomial equations. The typical setup is the following. Define

$$F : X \rightarrow \mathbb{C}^n : x \mapsto (f_1(x), \dots, f_n(x))$$

with $f_i \in R$. We want to compute $F^{-1}(0)$, that is, all points $x \in X$ such that $f_i(x) = 0, i = 1, \dots, n$. The homotopy approach to this problem is to construct $H : X \times \mathbb{C} \rightarrow \mathbb{C}^n$ such that $H_1 : x \mapsto H(x, 1)$ satisfies $Z_1 = H_1^{-1}(0) = F^{-1}(0)$ (the *target system* is equivalent to F) and the *start system* $G = H_0 : x \mapsto H(x, 0)$ is such that $Z_0 = G^{-1}(0)$ is easy to compute and contains the expected number δ of regular solutions. The number δ is equal to, for example, the Bézout number in the case of total degree homotopies, or the mixed volume of the Newton polytopes in the case of polyhedral homotopies [48, 27, 62]. Moreover, H has the additional property that $\Gamma : [0, 1) \rightarrow \mathbb{C} : s \mapsto s$ is a smooth parameter path. We denote

$$Z_0 = G^{-1}(0) = \{z_0^{(1)}, \dots, z_0^{(\delta)}\}$$

and by smoothness of Γ , we have that

$$Z_{t^*} = H_{t^*}^{-1}(0) = \{z_{t^*}^{(1)}, \dots, z_{t^*}^{(\delta)}\}$$

consists of δ distinct points in X for $t^* \in [0, 1)$ and the paths $\{(z_{t^*}^{(i)}, t^*), t^* \in [0, 1)\}$ are smooth and disjoint. Depending on the given system F , Z_1 may consist of fewer than δ points, or it might even consist of infinitely many points. Two or more paths may approach the same point as $t^* \rightarrow 1$ or paths may diverge to infinity. As stated in the introduction, several *end games* have been developed to deal with this kind of situations [28, 40, 41, 44]. We will focus here on the path tracking before the paths enter the end game operating region. We assume, for simplicity that this region is $[t_{EG}, 1]$, for t_{EG} a parameter value ‘near’ 1. Algorithm 1 is a simple template algorithm for smooth path tracking. With a slight abuse of notation, we use $z_{t^*}^{(i)}$ both for actual points on the path and ‘satisfactory’ numerical approximations of the $z_{t^*}^{(i)}$.

The algorithm uses several auxiliary procedures. The *predictor* (line 6) computes a point $\tilde{z} \in X$ and a stepsize Δt such that \tilde{z} is an approximation for $z_{t^* + \Delta t}^{(i)}$. Some existing predictors use an Euler step (tangent predictor) or higher order integrating techniques such as RK4². Intuitively, the computed

²Some higher order predictors need several previous points on the path in order to compute \tilde{z} . The predictor we present in this algorithm uses only the last computed point, hence the notation in Algorithm 1.

Algorithm 1 Template path tracking algorithm with a priori step control

```

1: procedure Track( $H, Z_0$ )
2:  $Z_1 \leftarrow \emptyset$ 
3: for  $z_0^{(i)} \in Z_0$  do
4:    $t^* \leftarrow 0$ 
5:   while  $t^* < t_{\text{EG}}$  do
6:      $(\tilde{z}, \Delta t) \leftarrow \text{predict}(H, z_{t^*}^{(i)}, t^*)$ 
7:      $z_{t^*+\Delta t}^{(i)} \leftarrow \text{correct}(H, \tilde{z}, t^* + \Delta t)$ 
8:      $t^* \leftarrow t^* + \Delta t$ 
9:   end while
10:   $z_1^{(i)} \leftarrow \text{endgame}(H, z_{t^*}^{(i)}, t^*)$ 
11:   $Z_1 \leftarrow Z_1 \cup \{z_1^{(i)}\}$ 
12: end for
13: return  $Z_1$ 
14: end procedure

```

stepsize Δt should be small in ‘difficult’ regions. Algorithms that take this into account are called *adaptive stepsize* algorithms. The main contribution of this paper is the adaptive stepsize predictor algorithm which we present in detail in Section 5. Our predictor computes an appropriate stepsize *before* the step is taken (a priori step control). The *corrector* step (line 7) then refines \tilde{z} to a satisfactory numerical approximation of $z_{t^*+\Delta t}^{(i)}$. Typically, satisfactory means that the relative backward error of $z_{t^*+\Delta t}^{(i)}$ is of size \pm the unit roundoff. The endgame procedure in line 10 finishes the path tracking by performing an appropriate end game.

3 Puiseux Series and Padé Approximants

In this section we introduce some aspects of Puiseux series solutions and Padé approximants that are relevant to this paper. References are provided for the reader who is interested in a more detailed treatment. In a first subsection we introduce Puiseux series. This will give us insight in the local behaviour of the fibers of π near singularities. In the rest of the section, we discuss Padé approximants with an emphasis on how they behave in the presence of this kind of singularities and present two illustrative examples. We point out that, since we assume smoothness of the path (as described in the previous section), we will not construct series approximations at singularities in our algorithm. The Padé approximant at a regular point is influenced by nearby singular points, and it can be used to estimate their location.

Let $\mathbb{C}[[t]]$ be the ring of formal power series in the variable t and let $\mathfrak{m} = \langle t \rangle$ be its maximal ideal. We denote $\mathbb{C}[t]_{\leq d} \simeq \mathbb{C}[[t]]/\mathfrak{m}^{d+1}$ for the \mathbb{C} -vector space of polynomials of degree at most d . For $f, g \in \mathbb{C}[[t]]$, the notation $f = g + O(t^{d+1})$ means that $f - g \in \mathfrak{m}^{d+1}$. The field of fractions of $\mathbb{C}[[t]]$ is denoted $\mathbb{C}(t)$.

3.1 Puiseux series

Let $R = \mathbb{C}[x_1^{\pm 1}, \dots, x_n^{\pm 1}]$ be the ring of Laurent polynomials in n variables and let $X = (\mathbb{C} \setminus \{0\})^n$ be the n -dimensional algebraic torus. We consider a homotopy given by $H(x, t) : X \times \mathbb{C} \rightarrow \mathbb{C}^n$:

$$H(x, t) = (h_1(x, t), \dots, h_n(x, t))$$

with $h_i \in R[t]$. We will denote

$$h_i = \sum_{\hat{q} \in \mathcal{A}_i} c_{\hat{q}} x^{\hat{q}} t^{k_{\hat{q}}}$$

where $\hat{q} = (q, k_q) \in \mathbb{Z}^n \times \mathbb{N}$ represents the exponent of a Laurent monomial in $R[t]$, $c_{\hat{q}} \in \mathbb{C}^*$ and $\mathcal{A}_i \subset \mathbb{Z}^n \times \mathbb{N}$ is the support of h_i . A *series solution at $t^* = 0$* of $H(x, t)$ is a parametrization of the form

$$\begin{cases} x_j(s) = a_j s^{\omega_j} (1 + \sum_{\ell=1}^{\infty} a_{j\ell} s^{\ell}), & j = 1, \dots, n \\ t(s) = s^m \end{cases} \quad (2)$$

with $m \in \mathbb{N} \setminus \{0\}$, $\omega = (\omega_1, \dots, \omega_n) \in \mathbb{Z}^n$, $a = (a_1, \dots, a_n) \in (\mathbb{C} \setminus \{0\})^n$, $a_{j\ell} \in \mathbb{C}$ and such that $H(x(s), t(s)) = H(x_1(s), \dots, x_n(s), t(s)) \equiv 0$ and there is a real $\epsilon > 0$ such that the series $x_i(s)$ converge for $0 < |s| \leq \epsilon$. Such a series representation can be found for all irreducible components of $Z = H^{-1}(0)$ intersecting but not contained in the hyperplane $\{t = 0\}$ (see for instance [28, 37, 38, 41]). Substituting (2) in a monomial of h_i we get

$$x(s)^q t(s)^{k_q} = a^q s^{\langle \omega, q \rangle + m k_q} (1 + O(s))$$

where $\langle \cdot, \cdot \rangle$ is the usual pairing in \mathbb{Z}^n . It follows that the lowest order term in the series $h_i(x(s), t(s))$ has exponent $\min_{\hat{q} \in \mathcal{A}_i} (\langle \omega, q \rangle + m k_q)$. Denoting $\hat{\omega} = (\omega, m) \in \mathbb{Z}^{n+1}$ and

$$\partial_{\hat{\omega}} \mathcal{A}_i = \{\hat{q} \in \mathcal{A}_i \mid \langle \hat{\omega}, \hat{q} \rangle = \min_{\hat{q} \in \mathcal{A}_i} (\langle \hat{\omega}, \hat{q} \rangle)\}, \quad \partial_{\hat{\omega}} h_i = \sum_{\hat{q} \in \partial_{\hat{\omega}} \mathcal{A}_i} c_{\hat{q}} x^q t^{k_q},$$

the vanishing of the lower order terms of $H(x(s), t(s))$ gives

$$\partial_{\hat{\omega}} h_i(a, 1) = \sum_{\hat{q} \in \partial_{\hat{\omega}} \mathcal{A}_i} c_{\hat{q}} a^q = 0, \quad i = 1, \dots, n.$$

We note three things.

1. The set $\partial_{\hat{\omega}} \mathcal{A}_i$ contains at least two exponents, since none of the $c_{\hat{q}}$ are zero and $a \in (\mathbb{C} \setminus \{0\})^n$. It follows that $\partial_{\hat{\omega}} \mathcal{A}_i$ corresponds to a positive dimensional face $\mathcal{F}_{\hat{\omega}}$ of the convex hull Q_i of \mathcal{A}_i . Since it is defined by $\hat{\omega} = (\omega, m)$ with $m \in \mathbb{N} \setminus \{0\}$, $\mathcal{F}_{\hat{\omega}}$ is contained in the *lower hull* of Q_i (the facet normal points in the positive t -direction).
2. The point $(a, 1) \in (\mathbb{C}^*)^{n+1}$ is a solution of the *face system* corresponding to $\hat{\omega}$:

$$\partial_{\hat{\omega}} h_1(a, 1) = \dots = \partial_{\hat{\omega}} h_n(a, 1) = 0.$$

3. The algorithm to compute more terms of the series is a generalization of the Newton-Puiseux procedure for algebraic plane curves and can be found, for instance, in [38].

For $t = 0$, $H_0 = H(x, 0)$ represents a square polynomial system in the x_i and a series solution at $t = 0$ corresponds to a solution $x(0)$ of this system. If $\omega = 0$, $H(a, 0) = 0$ and hence $a \in (\mathbb{C}^*)^n$ is a toric solution. If one of the coordinates of ω , say ω_j is nonzero, then $x_j(s)$ is either zero for $s = 0$ ($\omega_j > 0$) or escapes to infinity as $s \rightarrow 0$ ($\omega_j < 0$).

Remark 3.1. A series solution at $t = t^*$, $t^* \in \mathbb{C}$ of $H(x, t)$ can be obtained from a series solution around $t = 0$ of $G(x, t) = H(x, t + t^*)$. It satisfies $H(x(s), t(s)) = 0$ and has the form

$$\begin{cases} x_j(s) = a_j s^{\omega_j} (1 + \sum_{\ell=1}^{\infty} a_{j\ell} s^{\ell}), & j = 1, \dots, n \\ t(s) = t^* + s^m \end{cases}.$$

Substituting $s = t^{1/m}$ in the coordinate functions we get

$$x_j(t) = a_j t^{\omega_j/m} \left(1 + \sum_{\ell=1}^{\infty} a_{j\ell} t^{\ell/m} \right), \quad j = 1, \dots, n \quad (3)$$

which is a *Puiseux series* of order ω_j/m . We think of $x_j(t)$ as a function of a complex variable t , convergent by assumption in the punctured disk $0 < |t| \leq \epsilon^m$. Then $t^* = 0$ is either a regular point if (3) is a Taylor series, a pole if it is a Laurent series with strictly negative powers, or a branch point if non integer fractional powers occur. Since in a regular point t^* , the $x_j(t)$ are Taylor series, they will have convergence radii equal to the distance to the nearest singular point t_s . The corresponding series solution(s) of $H(x, t)$ around $t = t_s$ will give the type of singularity. The discussion in this subsection shows that $t = t_s$ is either a branch point or a pole.

Example 2. Consider the algebraic plane curve given by $H(x, t) = tx^3 + 2x^2 + t$. The Newton polygon is given in the left part of Figure 4. The faces of the lower hull are indicated with bold blue lines. The facet normals are also shown in the figure (not to scale). From the discussion above, the parameters of any series solution $(x(s), t(s))$ must be such that $x(s) = as^{\omega}(1 + O(s))$, $t(s) = s^m$ with $\hat{\omega} = (\omega, m)$ one such facet normal. Furthermore, the constant a must be a nonzero solution of the face system $\partial_{\hat{\omega}} H(a, 1) = 0$. For $\hat{\omega}_1 = (-1, 1)$, the face equation is $tx^3 + 2x^2 = 0$ with nonzero solution $a = -2$ for $t = 1$. We expect a series solution $x_1(t) = -2t^{-1} + O(1)$. There are no other nonzero solutions to the face equation, so we consider the next facet normal. The vector $\hat{\omega}_2 = (1, 2)$ gives face equation $2x^2 + 1$ with two nonzero solutions $\pm\sqrt{-2}/2$. This gives $x_2 = \sqrt{-2t}/2 + O(t)$ and $x_3 = -\sqrt{-2t}/2 + O(t)$. The real parts of the solution curves are shown in the right part of Figure 4.

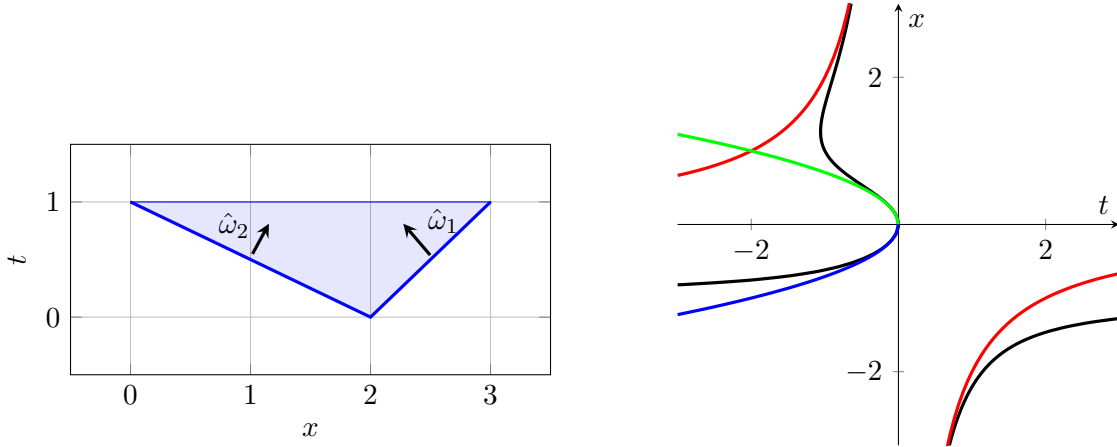


Figure 4: Left: Newton polygon of $H(x, t)$ from Example 2. Right: the curve $H(x, t) = 0$ (black), and the first term of the series expansions x_1 (red), x_2 (green) and x_3 (blue).

△

3.2 Padé approximants

In the rest of this section we discuss Padé approximants and the way they behave in the presence of poles and branch points. An extensive treatment of Padé approximants can be found in [3]. We will limit ourselves to the definition and the properties that are relevant to the heuristics of our algorithm.

The following definition uses some notation of [3].

Definition 3.2 (Padé approximant). Let $x(t) = \sum_{\ell=0}^{\infty} c_{\ell} t^{\ell} \in \mathbb{C}[[t]]$. The type (L, M) Padé approximant of $x(t)$ is

$$[L/M]_x = \frac{p(t)}{q(t)} \in \mathbb{C}(t)$$

such that $p(t) \in \mathbb{C}[t]_{\leq L}$ and $q(t) \in \mathbb{C}[t]_{\leq M}$ is a unit in $\mathbb{C}[[t]]$, with

$$[L/M]_x - x \in \mathfrak{m}^k \quad (4)$$

for k maximal.

Informally, Padé approximants are rational functions agreeing with the Maclaurin series of a function x up to a degree that is as large as possible. They are generalizations of truncated Maclaurin series, which are type $(L, 0)$ Padé approximants. Just like Maclaurin expansions are specific instances of Taylor expansions, it is straightforward to define Padé approximants around points $t = t^*$ in the complex plane different from 0. Without loss of generality, we consider only approximants around $t^* = 0$, since the general case reduces to this case after a simple change of coordinates. The type (L, M) Padé approximant is known to exist and it is unique. Multiplying the condition (4) by q yields

$$p(t) - x(t)q(t) \in \mathfrak{m}^k \quad \text{or equivalently,} \quad p(t) = x(t)q(t) + O(t^k) \quad (5)$$

for k maximal. Writing $p(t) = a_0 + a_1 t + \dots + a_L t^L$, $q(t) = b_0 + b_1 t + \dots + b_M t^M$ and equating terms of the same degree, this gives k linear conditions on the a_i , b_i , which can always be satisfied for $k \leq M + L + 1$. So for the linearized condition (5), k is at least $M + L + 1$. Computing the a_i and b_i in practice is a nontrivial task. Difficulties are, for instance, degenerate situations where $\deg(p) < L$ or $\deg(q) < M$ and the presence of so-called *Froissart doublets* (spurious pole-zero pairs [54, Chapter 27]). Some of the issues are discussed in [3, Chapter 2] and in [7, 25, 29]. In [25], a robust algorithm is proposed for computing Padé approximants. We will use this algorithm to compute Padé approximants from the coefficients c_i in our algorithm, presented in Section 5. The algorithm we use to compute the c_i is discussed in the next section.

What's important for our purpose is that a Padé approximant can be used to detect singularities of $x(t)$ of the types we are interested in (poles and branch points) close to $t^* = 0$, even for relatively small L and M . The idea is to compute Padé approximants of the coordinate functions $x_j(t)$ from local information on the path (the series coefficients c_{ℓ}) and use them as a *radar* for detecting difficulties near the path. We are now going to motivate this. Since we intend to use Padé approximants to detect only *nearby* singularities, a natural first class to consider is the type $(L, 1)$ approximants. We allow the approximant to have only one singularity, and hope that it chooses to place this singularity near the actual nearest singularity to capture the nearby non-analytic behaviour. Here is a powerful result due to Beardon [6].

Theorem 3.3. *Let $x_j(t)$ be analytic in $\{t^* \in \mathbb{C} \mid |t^*| \leq r\}$. An infinite subsequence of $\{[L/1]_{x_j}\}_{L=0}^{\infty}$ converges to $x_j(t)$ uniformly in $\{t^* \in \mathbb{C} \mid |t^*| \leq r\}$.*

Proof. We refer to [6] or [3, Theorem 6.1.1] for a proof. □

This applies in our case as follows. Suppose that $(a, 0) \in X \times \mathbb{C}$ is a regular point of the variety $Z = H^{-1}(0)$ and the irreducible component of Z containing $(a, 0)$ is not contained in $\{(x, t^*) \in X \times \mathbb{C} \mid t^* = 0\}$. Then there is a holomorphic function $x : \mathbb{C} \rightarrow X$ such that $x(0) = a$ and $H(x(t^*), t^*) = 0$ for t^* in some nonempty open neighborhood of 0 (see for instance Theorem A.3.2 in [48]). That is, if a is a regular solution of H_0 , then the corresponding power series solution (2) consists of n Taylor series $x_j(t)$. The function $x(t)$ can be continued analytically in a disk with radius r if no

singularities lie within a distance r from the origin. Theorem 3.3 makes the following statement precise. For large enough degrees L of the numerator of the Padé approximant, the $[L/1]_{x_j}$ are expected to approximate the coordinate functions $x_j(t)$ in a disk centered at the origin with radius \pm the distance to the most nearby singularity. The fact that for sufficiently large L , the pole of $[L/1]_{x_j}$ is expected to give an indication of the *distance* to the nearest singularity (also if it is a branch point) can be seen as follows. Write $x_j(t) = \sum_{\ell=0}^{\infty} c_{\ell} t^{\ell}$ for the Maclaurin expansion of the coordinate function $x_j(t)$. Then a simple computation shows that if $c_L \neq 0$,

$$[L/1]_{x_j} = c_0 + c_1 t + \dots + c_{L-1} t^{L-1} + \frac{c_L t^L}{1 - c_{L+1} t / c_L}.$$

Hence the pole of $[L/1]_{x_j}$ is c_L / c_{L+1} (or it is ∞ if $c_{L+1} = 0$). For large L , the modulus $|c_L / c_{L+1}|$ can be considered an approximation of the limit

$$\lim_{L \rightarrow \infty} \left| \frac{c_L}{c_{L+1}} \right|$$

if this limit exists. Also, if this limit exists it is a well known expression for the convergence radius of the power series $x_j(t) = \sum_{\ell=0}^{\infty} c_{\ell} t^{\ell}$, which is the distance to the nearest singularity. Since the main application we have in mind is polynomial system solving, in which the homotopy is usually ‘randomized’, in practice this limit exists and for reasonably small L , $|c_L / c_{L+1}|$ is a satisfactory approximation of the convergence radius of the power series. Theorem 3.3 suggests that more is true: it can be expected that the ratio c_L / c_{L+1} is a reasonable estimate for the actual location of the most nearby singularity. This is Fabry’s ratio theorem [20]; see also [9, 18, 51].

Theorem 3.4. *If the coefficients of the power series $x_j(t) = \sum_{\ell=0}^{\infty} c_{\ell} t^{\ell}$ satisfy $\lim_{L \rightarrow \infty} c_L / c_{L+1} = t_s$, then $t = t_s$ is a singular point of the sum of this series. The point $t = t_s$ belongs to the boundary of the circle of convergence of the series.*

Proof. See [20]. □

We now briefly discuss the behaviour of type (L, M) Padé approximants in the presence of poles and branch points and end the section with two illustrative examples.

3.3 Padé approximants and nearby poles

Since Padé approximants are rational functions, it is reasonable to expect that they can capture this kind of behaviour quite well. The following theorem, due to de Montessus [16], gives strong evidence of this intuition.

Theorem 3.5. *Suppose $x_j(t)$ is meromorphic in the disk $\{t^* \in \mathbb{C} \mid |t^*| \leq r\}$, with μ distinct poles $z_1, \dots, z_{\mu} \in \mathbb{C}$ in the punctured disk $\{t^* \in \mathbb{C} \setminus \{0\} \mid |t^*| < r\}$. Furthermore, suppose that m_i is the multiplicity of the pole z_i and $\sum_{i=1}^{\mu} m_i = M$. Then $\lim_{L \rightarrow \infty} [L/M]_{x_j} = x_j$ on any compact subset of $\{t^* \in \mathbb{C} \mid |t^*| \leq r, t^* \neq z_i, i = 1, \dots, \mu\}$.*

Proof. This is Theorem 6.2.2 in [3]. □

Loosely speaking, this tells us that the poles of $[L/M]_{x_j}$, for large enough L , will converge to the M most nearby poles of $x_j(t)$ (counting multiplicities), if these are the only singularities encountered in the disk $\{t^* \in \mathbb{C} \mid |t^*| \leq r\}$. For the $[L/1]_{x_j}$ approximant, this means that convergence may be expected beyond the nearest singularity if this is a simple pole, and the pole of $[L/1]_{x_j}$ will approximate the actual nearby pole. This may be considered as a practical approach to analytic continuation [55]. Padé approximants also give answers to the inverse problem: the asymptotic behaviour of the poles of $[L/M]_{x_j}$ as $L \rightarrow \infty$ can be used to describe meromorphic continuations of the function $x_j(t)$. We do not give any details here, the interested reader is referred to [24, 50, 59].

3.4 Padé approximants and nearby branch points

Many singularities encountered in polynomial homotopy continuation are not poles, but branch points. This situation is more subtle since the Padé approximant, being a rational function, cannot have branch points. For an intuitive description of the behaviour of Padé approximants for functions with multi-valued continuations, the reader may consult [3, Section 2.2]. The conclusion is that the poles and zeros of $[L/M]_{x_j}$ are expected to delineate a ‘natural’ branch cut. The authors also describe some ways to estimate the location and winding number of branch points using Padé approximants. We should also mention that there are convergence results in the presence of branch points which involve potential theory. We refer to [49] for some important results for convergence of sequences of Padé approximants with $L, M \rightarrow \infty$, $L/M \rightarrow 1$ (so-called *near-diagonal* sequences). These results are beyond the scope of this paper, mainly because we will limit ourselves to *near-polynomial* approximants: we allow only a small number of poles (often we even take $M = 1$) and we will estimate nearby singularities directly from $[L/M]_{x_j}$. This is an unusual choice, since near-diagonal approximants tend to show better behavior for the approximation of algebraic functions (see, e.g. [42, Section 6.2]). The reason for this choice will become clear from the example in Section 3.5.2.

We will show in experiments that in this way, even for small L , we can predict at least the order of magnitude of the distance to the nearest branch point, which is enough to ring an alarm when this distance gets small, and often we can do much better.

The reason for limiting ourselves to a small number of parameters $L + M$ and for not trying to compute a very accurate location of the nearest branch point and its winding number is of course efficiency. Moreover, for the purpose of this paper a local approximation of the coordinate functions and a rough estimate of the nearest singularity suffice. The above mentioned techniques to compute more information about nearby branch points may be powerful for approximation of algebraic curves in compact regions of the complex plane and for computing monodromy groups. We leave this as future research.

3.5 Examples

Our first example shows the potential of using Padé approximants for locating nearby singularities in the parameter space. The second one motivates the choice of type $(L, 1)$ approximants over near-diagonal approximants.

3.5.1 Padé approximants for a family of hyperbolas

We consider again the homotopy (1) from Example 1. Let us first take $p = 0.19$ and consider the smooth parameter path Γ_3 . It is clear that the singularity $z_+ = 1/2 + p\sqrt{-1} \in S$ is the closest singularity to nearly every point in $\Gamma_3([0, 1])$. As s moves closer to $1/2$, it moves closer to z_+ . To show how this causes difficulties for the local approximation using Padé approximants, we have performed the following experiment. For several points t^* on the parameter path $\Gamma_3([0, 1])$ we have plotted the contour in \mathbb{C} where the absolute value of the difference between $x(t) = \sqrt{(t - 1/2)^2 + p^2}$ and its type $(6, 1)$ Padé approximation around t^* equals 10^{-4} . The result is shown in Figure 5. It is clear that the local approximation can be ‘trusted’ in a much larger region if the singularity is far away.

We now investigate the behaviour of the pole of $[L/1]_x$ as we move along the path. We consider the four cases defined by $p = 0.15, 0.19$ and $L = 2, 6$. The results are shown in Figure 6. The figure shows that as we move closer to $\Gamma(0.5)$ on the path, the pole of the Padé approximant moves closer to the actual branch point. What’s important is that in the trouble region of the path (s close to 0.5), the pole of $[L/1]_x$ is fairly close to z_+ . It gives, at least, an indication of the order of magnitude of the distance to z_+ . Another way to see this is that on a point of the path near to z_+ , the $(L, 1)$ Padé approximant is not so much influenced by the presence of z_- . For instance, at $t^* = 0$, the pole is

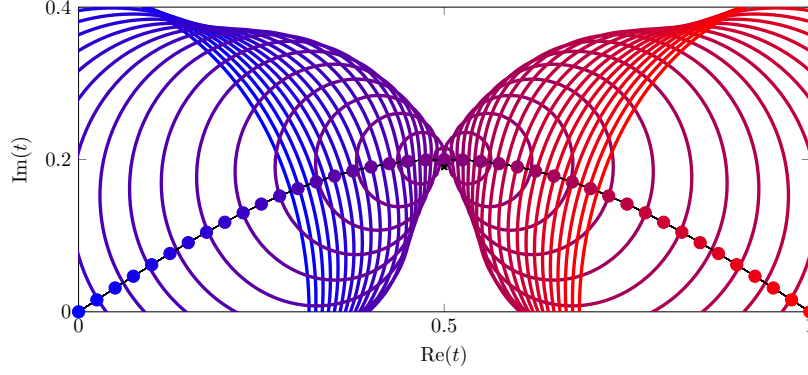


Figure 5: Contours of the approximation error as described in Section 3.5.1. The colour of the contours correspond to the colour of the dots on the parameter path they correspond to. The singularity z_+ is shown as a small black cross.

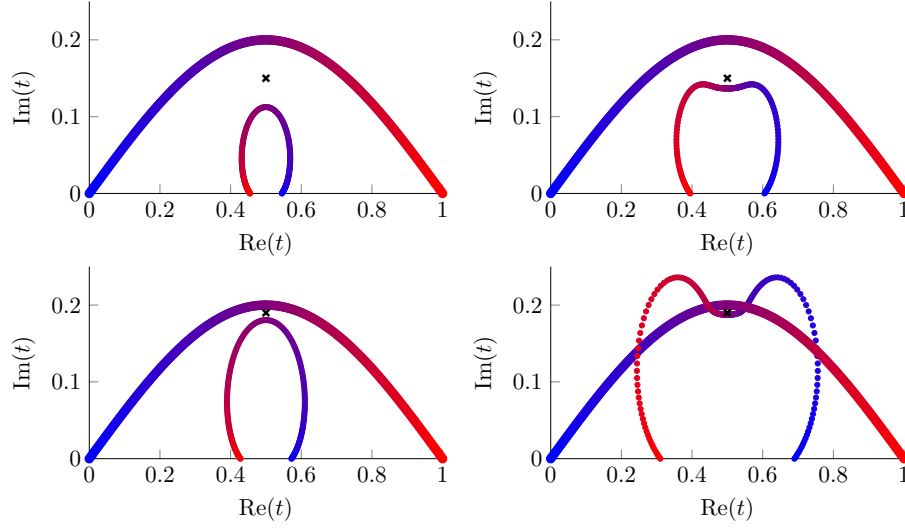


Figure 6: The path $\Gamma_3([0, 1])$ and the corresponding path described by the pole of the type $(L, 1)$ Padé approximant (associated points on the two paths have been given the same colour) for $p = 0.15$ (first row), $p = 0.19$ (second row), $L = 2$ (left column), $L = 6$ (right column).

real because z_+ and z_- are complex conjugates and they are located at the same distance from $\Gamma_3(0)$. For t^* near $\Gamma_3(0.5)$, the pole has a relatively large positive imaginary part. Comparing the first row to the second row in the figure shows that this effect gets stronger when a singularity moves closer to the path. Comparing the left column to the right column we see that the approximation of z_+ gets better as L increases, which is to be expected. If we use Γ_1 instead of Γ_3 , for whatever p , the branch points z_+ and z_- will have the same distance to each point of the path. The result is that the $(L, 1)$ Padé approximant will have poles on the real line. For $L = 4$, $p = 0.001$, $t^* \in [0, 1]$, the pole is contained in the real interval $[0.4997, 0.5003]$, so the local difficulties are detected. However, in this specific situation, it is more natural to use type $(L, 2)$ approximants. The result for $L = 6$, $p = 0.05$ is shown in Figure 7. We note that in a randomized homotopy, it is not to be expected that at a general point of the path two poles are equally important. As we move along the path, the most important singularity may change, and the type $(L, 1)$ approximant can be expected to relocate its pole accordingly.

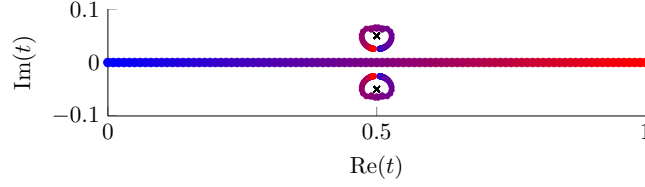


Figure 7: The path $\Gamma_1([0, 1])$ and the corresponding paths described by the poles of the type $(6, 2)$ Padé approximant (associated points on the two paths have been given the same colour) for $p = 0.05$.

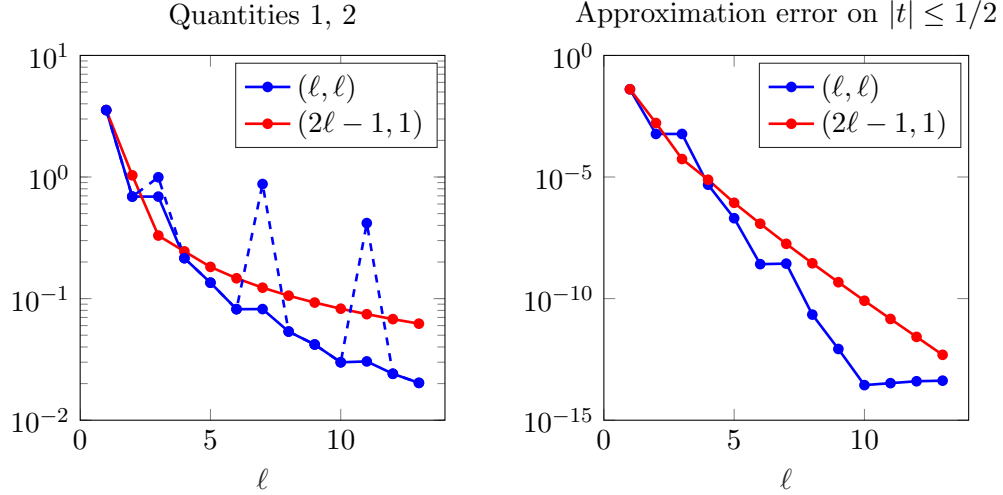


Figure 8: Results of the experiment in Section 3.5.2.

3.5.2 Near-diagonal VS near-polynomial approximants

Consider the algebraic function $x(t) = \sqrt{(t + 1.01)(t^2 - t + 37/4)}$ with branch points

$$S = \{-1.01, 1/2 + 3\sqrt{-1}, 1/2 - 3\sqrt{-1}\}.$$

For $\ell = 1, \dots, 13$, we compute both the type (ℓ, ℓ) and the type $(2\ell - 1, 1)$ Padé approximant (around $t = 0$) of $x(t)$ using a Matlab implementation of the algorithm in [25]. For all these approximants we compute

1. the minimum of the distances of the poles of the Padé approximant to the branch point -1.01 ,
2. the difference between the smallest modulus of the poles of the Padé approximant and the modulus of the nearest branch point, which is 1.01 ,
3. an estimate for the approximation error (the infinity norm of a discretized approximation) of $x(t)$ on the disk $|t| \leq 1/2$ in the complex plane.

Results are shown in Figure 8. The right part of the figure shows that the diagonal approximants behave better for function approximation. However, for small ℓ , the near-polynomial approximants are competitive. For the type $(2\ell - 1, 1)$ approximant, the first two quantities coincide since the pole is real. For the (ℓ, ℓ) case, the first quantity is a lower bound for the second one. This is illustrated by the difference between the dashed and the full blue line in Figure 8. What happens is the following. One of the poles of the type (ℓ, ℓ) approximant approximates the branch point -1.01 , but some other pole indicates that there could be a branch point with smaller modulus. This is illustrated in Figure

9 for $\ell = 3, 4$ (for $\ell = 4$, one of the poles of the (ℓ, ℓ) approximant lies close to that of the $(2\ell - 1, 1)$ approximant and the corresponding dot is nearly invisible). The pole of the type $(3, 3)$ approximant that is closest to the origin actually comes from a Froissart doublet which was not detected using the default settings in the algorithm of [25]. As a consequence, this spurious pole would tell us that a singularity is nearby such that only a small step can be taken (see Section 5.1.3), while the actual branch point is quite far away. Detecting such Froissart doublets is often tricky. Since we will use only low orders, the approximation quality of the $(L, 1)$ approximant suffices for our purpose. Moreover, this example shows that they are more robust for estimating the distance to the nearest singularity. We will use this type of approximants for our default settings.

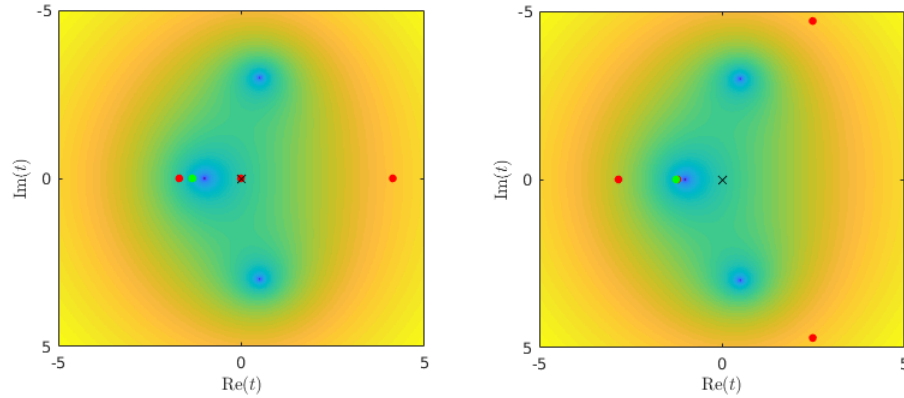


Figure 9: Poles of the type (ℓ, ℓ) approximant (red dots) and pole of the type $(2\ell - 1, 1)$ approximant (green dot) for $\ell = 3, 4$ (left and right respectively). The origin is indicated with a black cross. The background color corresponds to $|x(t)|$.

4 Computing Power Series Solutions

In this section we present the algorithm for computing a power series solution of $H(x, t)$ at $t^* = 0$ proposed in [10] and prove a result of convergence. An analogous result for the case $n = 1$ can be found in [36]. We will consider the situation where the series solution has the form (2) with parameters satisfying $\omega_i \geq 0$. Furthermore, we assume that the winding number m is known. If this is not the case, m can be computed by using, for instance, monodromy loops. Note that it is sufficient to consider the case where $m = 1$, since if m is known and $m > 1$ we can consider the homotopy

$$\hat{H}(x, \tau) = (h_1(x, \tau^m), \dots, h_n(x, \tau^m))$$

with power series solution

$$\begin{cases} x_j(s) = a_j s^{\omega_j} (1 + \sum_{\ell=1}^{\infty} a_{j\ell} s^{\ell}), & j = 1, \dots, n \\ \tau(s) = s \end{cases}.$$

Therefore, we can avoid introducing the extra parameter s and the unknown power series solution is given by

$$x_j(t) = a_j t^{\omega_j} \left(1 + \sum_{\ell=1}^{\infty} a_{j\ell} t^{\ell} \right), j = 1, \dots, n. \quad (6)$$

We think of $H(x, t)$ as a column vector $[h_1 \cdots h_n]^\top$ in $R[[t]]^n \simeq R^n[[t]]$ and the Jacobian matrix $J_H(x, t)$ is considered an element of $R[[t]]^{n \times n} \simeq R^{n \times n}[[t]]$. For any $h(x, t) \in R[[t]]^n$, plugging in $y(t) \in \mathbb{C}[[t]]^n$ gives $h(y(t), t) \in \mathbb{C}[[t]]^n$, and the same can be done for $J(x, t) \in R[[t]]^{n \times n}$, which gives $J(y(t), t) \in \mathbb{C}[[t]]^{n \times n}$.

Definition 4.1. Let \star be either \mathbb{C}^n or $\mathbb{C}^{n \times n}$. For $v = \sum_{\ell=0}^{\infty} v_\ell t^\ell \in \star[[t]] \setminus \{0\}$, the order of v is

$$\text{ord}(v) = \min_{\ell} \{v_\ell \neq 0\},$$

where $v_\ell \in \star, \ell \in \mathbb{N}$. For $w \neq v \in \star[[t]]$ we denote $v = w + O(t^k)$ if $\text{ord}(v - w) \geq k$. For $v = 0$, we define $\text{ord}(v) = \infty$.

Note that this means that for a vector or matrix v with power series entries $v = O(t^k)$ if and only if every entry of v is in \mathfrak{m}^k , where \mathfrak{m} is the maximal ideal of $\mathbb{C}[[t]]$. With elementwise addition and multiplication in $\mathbb{C}[[t]]^n$ and the usual addition and multiplication in $\mathbb{C}[[t]]^{n \times n}$, it is clear that for $v, w \in \star[[t]]$, $\text{ord}(v) = \text{ord}(-v)$, $\text{ord}(v + w) \geq \min(\text{ord}(v), \text{ord}(w))$ and $\text{ord}(vw) \geq \text{ord}(v) + \text{ord}(w)$. For the product rule, equality holds if $\star = \mathbb{C}^n$. Matrix-vector multiplication $\mathbb{C}[[t]]^{n \times n} \times \mathbb{C}[[t]]^n \rightarrow \mathbb{C}[[t]]^n$ is defined in the usual way and for $M \in \mathbb{C}[[t]]^{n \times n}, v \in \mathbb{C}[[t]]^n$ we have $\text{ord}(Mv) \geq \text{ord}(M) + \text{ord}(v)$.

Given $x^{(0)}(t) = (x_1^{(0)}(t), \dots, x_n^{(0)}(t)) \in \mathbb{C}[[t]]^n$, fix positive integers $w_k \in \mathbb{N} \setminus \{0\}$ and consider the sequence $\{x^{(k)}(t)\}_{k \geq 0}$ defined by

$$\begin{aligned} \tilde{x}^{(k+1)}(t) &= x^{(k)}(t) - J_H(x^{(k)}(t), t)^{-1} H(x^{(k)}(t), t) = \sum_{\ell=0}^{\infty} b_\ell t^\ell, \\ x^{(k+1)}(t) &= \sum_{\ell=0}^{w_k-1} b_\ell t^\ell \end{aligned} \tag{7}$$

where we assume that $J_H(x^{(k)}(t), t)$ is a unit in $\mathbb{C}[[t]]^{n \times n}$ for all k and this is equivalent to assuming that $J_H(x^{(k)}(0), 0) \in \text{GL}(n, \mathbb{C})$ for all $k \geq 0$. The iteration is clearly based on the well known Newton-Raphson iteration for approximating a root of a nonlinear system of equations. The following theorem specifies the statement that the iteration has similar ‘quadratic’ convergence properties. It is related to a multivariate version of Hensel lifting, see for instance [19, Exercise 7.26].

Theorem 4.2. Let $H(x, t) : X \times \mathbb{C} \rightarrow \mathbb{C}$ be a homotopy with power series solution $x(t) \in \mathbb{C}[[t]]^n$ given by (6) and let $\{x^{(k)}(t)\}_{k \geq 0}$ be a sequence generated as in (7). If $J_H(x^{(k)}(t), t)$ is a unit in $\mathbb{C}[[t]]^{n \times n}$ for all $k \geq 0$ then

$$\text{ord}(x^{(k+1)}(t) - x(t)) \geq \min(2\text{ord}(x^{(k)}(t) - x(t)), w_k), \quad k \geq 0.$$

Proof. We know that $x(t) = (x_1(t), \dots, x_n(t))^\top \in \mathbb{C}[[t]]^n$ satisfies $H(x(t), t) = 0$. Take $x^{(k)}(t) \in \mathbb{C}[[t]]^n$ and define $e^{(k)}(t) = x^{(k)}(t) - x(t)$. We have

$$0 = H(x^{(k)}(t) - e^{(k)}(t), t) = H(x^{(k)}(t), t) - J_H(x^{(k)}(t), t)e^{(k)}(t) + O(t^{2\text{ord}(e^{(k)}(t))}). \tag{8}$$

By assumption, $J_H(x^{(k)}(t), t)$ is a unit and thus $\text{ord}(J_H(x^{(k)}(t), t)^{-1}) = 0$. We now multiply (8) from the left with $J_H(x^{(k)}(t), t)^{-1}$ and we get (using $e^{(k)}(t) = x^{(k)}(t) - x(t)$)

$$-J_H(x^{(k)}(t), t)^{-1} H(x^{(k)}(t), t) + (x^{(k)}(t) - x(t)) = O(t^{2\text{ord}(e^{(k)}(t))}).$$

It follows that $\tilde{x}^{(k+1)}(t) - x(t) = O(t^{2\text{ord}(e^{(k)}(t))})$. So we find that

$$\text{ord}(e^{(k+1)}(t)) \geq \min(2\text{ord}(e^{(k)}(t)), w_k).$$

□

It follows that if $e^{(0)}(t)$ has order ≥ 1 , the iteration converges to the solution $x(t)$ and the order of the error doubles in every iteration, as long as the truncation orders w_k allow for it. Also, if $\text{ord}(e^{(0)}(t)) \geq 1$, $H(x^{(0)}(0), 0) = 0$ and thus $\text{ord}(H(x^{(0)}(t), t)) \geq 1$. It follows that the term $-J_H(x^{(k)}(t), t)^{-1}H(x^{(k)}(t), t)$ has order at least 1 and so the constant terms of $x^{(1)}$ and $x^{(0)}$ agree. This stays true for the following iterations as well. We conclude that if $\text{ord}(e^{(0)}(t)) \geq 1$, the assumption that $J_H(x^{(k)}(t), t)$ is a unit for all k translates to the assumption that $x^{(0)}(0) = a$ is a regular solution of the polynomial system defined by H_0 . If we want to compute a series solution that is accurate up to order w , and $\text{ord}(e^{(0)}(t)) = r \geq 1$, we set $w_k = \min(r2^k, w)$ and execute $\lceil \log_2(w/r) \rceil$ steps of the iteration. We denote

$$\begin{aligned} J_H(x^{(k)}(t), t) &= J_0^{(k)} + J_1^{(k)}t + J_2^{(k)}t^2 + \dots, \\ H(x^{(k)}(t), t) &= H_0^{(k)} + H_1^{(k)}t + H_2^{(k)}t^2 + \dots, \\ \Delta x^{(k)}(t) &= -J_H(x^{(k)}(t), t)^{-1}H(x^{(k)}(t), t) = d_0^{(k)} + d_1^{(k)}t + d_2^{(k)}t^2 + \dots \end{aligned}$$

We have to compute the first w_k terms of $\tilde{x}^{(k+1)}(t) = x^{(k)}(t) + \Delta x^{(k)}(t)$. The equation

$$-J_H(x^{(k)}(t), t)\Delta x^{(k)}(t) = H(x^{(k)}(t), t) \quad (9)$$

gives

$$\begin{aligned} J_0^{(k)}d_0^{(k)} &= -H_0^{(k)}, \\ J_0^{(k)}d_1^{(k)} + J_1^{(k)}d_0^{(k)} &= -H_1^{(k)}, \\ J_0^{(k)}d_2^{(k)} + J_1^{(k)}d_1^{(k)} + J_2^{(k)}d_0^{(k)} &= -H_2^{(k)}, \\ &\vdots \\ J_0^{(k)}d_{w_k-1}^{(k)} + J_1^{(k)}d_{w_k-2}^{(k)} + \dots + J_{w_k-1}^{(k)}d_0^{(k)} &= -H_{w_k-1}^{(k)}. \end{aligned}$$

It is an immediate corollary from Theorem 4.2 that if $\text{ord}(e^{(0)}(t)) = r \geq 1$, then $d_i^{(k)} = 0, i = 0, \dots, w_k-1$ and hence $H_i^{(k)} = 0, i = 0, \dots, w_k-1$. It follows that we only have to solve

$$\begin{aligned} J_0^{(k)}d_{w_k-1}^{(k)} &= -H_{w_k-1}^{(k)}, \\ &\vdots \\ J_0^{(k)}d_{w_k-1}^{(k)} + J_1^{(k)}d_{w_k-2}^{(k)} + \dots + J_{w_k-w_k-1}^{(k)}d_{w_k-1}^{(k)} &= -H_{w_k-1}^{(k)}. \end{aligned} \quad (10)$$

and this can be done equation by equation, via backsubstitution. In practice, we will use these results as in Algorithm 2, where we assume that $r = 1, t^* \in \mathbb{C}, x^{(0)} \in \mathbb{C}^n \subset \mathbb{C}[[t]]^n$ such that $H(x^{(0)}, t^*) = 0$.

5 A Robust Algorithm for Tracking Smooth Paths

In this section we show how the results of the previous sections lead to a smooth path tracking algorithm. More specifically, we propose a new adaptive stepsize predictor for homotopy path tracking. We will use $\Gamma(s) = s$ and assume that this is a smooth parameter path for simplicity, but the generalization to different parameter paths is straightforward. The aim of this section is to motivate the heuristics and to present and analyze the algorithm. In the next section we will show some convincing experiments.

We will use Padé approximants for the prediction. The stepsize computation is based on two criteria. That is, we compute two candidate stepsizes $\{\Delta t_1, \Delta t_2\}$ based on two different estimates

Algorithm 2 Computes the powerseries solution of $H(x, t) = 0$ corresponding to $x^{(0)}$ around $t = t^*$.

```

1: procedure ComputeSeries( $H, t^*, w, x^{(0)}$ )
2:  $H \leftarrow H(x, t + t^*)$ 
3:  $k \leftarrow 0$ 
4: while  $k < \lceil \log_2(w) \rceil$  do
5:    $w_k \leftarrow \min(2^k, w)$ 
6:   Compute  $x^{(k+1)}$  by solving (10)
7:    $k \leftarrow k + 1$ 
8: end while
9: return  $\{x_1^{(k)}(t), \dots, x_n^{(k)}(t)\}$ 
10: end procedure

```

of the largest ‘safe’ stepsize. The eventual value of Δt that is returned by the predictor (line 6 in Algorithm 1) is $\min\{\Delta t_1, \Delta t_2, t_{\text{EG}} - t^*\}$. For the first criterion we estimate the distance to the nearest point of a different path in $X \times \{t^*\}$. This estimate is only accurate if we are actually in a difficult region. Comparing this to an estimate for the Padé approximation error we compute Δt_1 such that the predicted point \tilde{z} is much closer to the correct path than to the nearest different path. The value of Δt_2 is an estimate for the radius of the ‘trust region’ of the Padé approximant, which is influenced by nearby singularities in the parameter space (see Section 3). We discuss these two criteria in detail in the first subsection. In the second subsection we present the algorithm. In the last subsection we present a complexity analysis of our algorithm.

5.1 Adaptive stepsize: two criteria

The values of Δt_1 and Δt_2 are computed from an estimate of the distance to the nearest different path, the approximation error of the Padé approximant for small stepsizes and an estimate for some global ‘trust radius’ of the Padé approximants. We discuss these estimates first and then turn to the computation of Δt_1 and Δt_2 from these estimates.

5.1.1 Distance to the nearest path

We will use $\|\cdot\|$ to denote the euclidean 2-norm for vectors and the induced operator norm for matrices. Consider the homotopy $H : X \times \mathbb{C} \rightarrow \mathbb{C}^n$. Suppose that for some $t^* \in [0, 1)$ we have $H(z_{t^*}^{(1)}, t^*) = H(z_{t^*}^{(2)}, t^*) = 0$, so $z_{t^*}^{(1)} \neq z_{t^*}^{(2)} \in Z_{t^*}$ lie on two different solution paths. We assume that $z_{t^*}^{(1)}$ is close to $z_{t^*}^{(2)}$. Denote $\Delta z = z_{t^*}^{(2)} - z_{t^*}^{(1)} \in \mathbb{C}^n$ and think of Δz as a column vector. Our goal here is to estimate $\|\Delta z\|$. Neglecting higher order terms, we get

$$H(z_{t^*}^{(2)}, t^*) \approx H(z_{t^*}^{(1)}, t^*) + J_H(z_{t^*}^{(1)}, t^*)\Delta z + \frac{v}{2}, \quad v = \begin{bmatrix} \langle \mathcal{H}_1(z_{t^*}^{(1)}, t^*)\Delta z, \Delta z \rangle \\ \vdots \\ \langle \mathcal{H}_n(z_{t^*}^{(1)}, t^*)\Delta z, \Delta z \rangle \end{bmatrix} \quad (11)$$

where $(\mathcal{H}_i(x, t))_{j,k} = \frac{\partial^2 h_i}{\partial x_j \partial x_k}$, $1 \leq j, k \leq n$, are the Hessian matrices of the individual equations and $\langle \cdot, \cdot \rangle$ is the usual inner product in \mathbb{C}^n . To simplify the notation, we denote $\mathcal{H}_i = \mathcal{H}_i(z_{t^*}^{(1)}, t^*)$ and $J_H = J_H(z_{t^*}^{(1)}, t^*)$. The Hessian matrices are Hermitian, so they have a unitary diagonalization $\mathcal{H}_i = V_i \Lambda_i V_i^H$ where \cdot^H is the Hermitian transpose and the V_i are unitary matrices with eigenvectors of \mathcal{H}_i in their columns. We may write $\Delta z = V_i w_i$ for some coefficient vector w_i such that $\|w_i\| = \|\Delta z\|$. We have $\langle \mathcal{H}_i \Delta z, \Delta z \rangle = \langle \Lambda_i w_i, w_i \rangle$. Let $\sigma_{k,\ell} = \sigma_\ell(\mathcal{H}_k)$ be the ℓ -th singular value of \mathcal{H}_k . The absolute values of the

diagonal entries of Λ_i are exactly the singular values, so that $|\langle \mathcal{H}_i \Delta z, \Delta z \rangle| \leq \sigma_{i,1} \|w_i\|^2 = \sigma_{i,1} \|\Delta z\|^2$. It follows easily that $\|v\| \leq \sqrt{\sigma_{1,1}^2 + \dots + \sigma_{n,1}^2} \|\Delta z\|^2$. Since $\|J_H \Delta z\| \geq \sigma_n(J_H) \|\Delta z\|$ and by (11) we have $\|J_H \Delta z\| \approx \|v\|/2$, it follows that

$$\|\Delta z\| \gtrsim 2\sigma_n(J_H)(\sigma_{1,1}^2 + \dots + \sigma_{n,1}^2)^{-\frac{1}{2}}. \quad (12)$$

Intuitively, the ‘more regular’ the Jacobian, the better and the more curvature, the worse. Motivated by (12), we make the following definition.

Definition 5.1. For $z_{t^*}^{(i)} \in Z_{t^*}, t^* \in [0, 1)$, set $J_H = J_H(z_{t^*}^{(i)}, t^*)$ and $\sigma_{k,\ell} = \sigma_\ell(\mathcal{H}_k(z_{t^*}^{(i)}, t^*))$ and define $\eta_{i,t^*} = 2\sigma_n(J_H)(\sigma_{1,1}^2 + \dots + \sigma_{n,1}^2)^{-\frac{1}{2}}$.

The numbers η_{i,t^*} are estimates for the distance to the most nearby different path. To make sure the prediction error $\|x(t^* + \Delta t) - \tilde{x}(t^* + \Delta t)\|$ (where $\tilde{x}(t)$ is the coordinatewise Padé approximant) is highly unlikely to cause path jumping, we will solve $\|x(t^* + \Delta t) - \tilde{x}(t^* + \Delta t)\| = \beta_1 \eta_{i,t^*}$ for a small fraction $0 < \beta_1 \ll 1$ to compute an adaptive stepsize Δt . We now discuss how to estimate $\|x(t^* + \Delta t) - \tilde{x}(t^* + \Delta t)\|$.

5.1.2 Approximation error of the Padé approximant

Without loss of generality, we take the current value of t to be zero and consider Padé approximants around $t^* = 0$ as in Section 3. Suppose that we have computed a type (L, M) Padé approximant $[L/M]_{x_j} = p_j(t)/q_j(t)$ of a coordinate function $x_j(t)$ around 0. Given a small real stepsize Δt , we want to estimate the error

$$|e_j(\Delta t)| = \left| \frac{p_j(\Delta t)}{q_j(\Delta t)} - x_j(\Delta t) \right| = \left| \frac{a_0 + a_1 \Delta t + \dots + a_L \Delta t^L}{b_0 + b_1 \Delta t + \dots + b_M \Delta t^M} - x_j(\Delta t) \right|. \quad (13)$$

From Definition 3.2 we know that $e_j(t) \in \mathfrak{m}^k$ (where usually $k = L + M + 1$), so (13) can be written as $|e_{0,j} \Delta t^k + e_{1,j} \Delta t^{k+1} + \dots|$ with $e_{0,j} \neq 0$. For small Δt , the first term is expected to dominate the sum and so $|e_j(\Delta t)| \approx |e_{0,j} \Delta t^k|$. This estimate is also used in [22] for the case $L = 2, M = 1$ and a similar strategy is common to estimate the error in a power series approximation. An alternative is to use an estimate for the ‘linearized’ error

$$|q_j(\Delta t) e_j(\Delta t)| = |p_j(\Delta t) - x_j(\Delta t) q_j(\Delta t)| \quad (14)$$

which is equal to

$$|(b_0 + b_1 \Delta t + \dots + b_M \Delta t^M)(e_{0,j} \Delta t^k + e_{1,j} \Delta t^{k+1} + \dots)| \approx |b_0 e_{0,j} \Delta t^k|.$$

Since $q_j(t)$ is a unit in $\mathbb{C}[[t]]$, $b_0 \neq 0$ and we can scale p_j and q_j such that $b_0 = 1$ and the estimates of (13) and (14) coincide. Taking $b_0 = 1$, the constant $e_{0,j}$ is the coefficient of t^k in $(a_0 + a_1 t + \dots + a_L t^L) - (1 + b_1 t + \dots + b_M t^M)(c_0 + c_1 t + \dots)$, which is easily seen to be

$$e_{0,j} = a_k - (c_k + b_1 c_{k-1} + \dots + b_M c_{k-M}) \quad (15)$$

where $a_k = 0$ if $k > L$ and $c_j = 0$ for $j < 0$. Doing this for all j and assuming that k is the same for all coordinates we get an estimate

$$\left\| x(\Delta t) - \left(\frac{p_1(\Delta t)}{q_1(\Delta t)}, \dots, \frac{p_n(\Delta t)}{q_n(\Delta t)} \right) \right\| \approx \|e_0\| |\Delta t|^k, \quad (16)$$

with $e_0 = (e_{0,1}, \dots, e_{0,n})$.

5.1.3 Trust region for the Padé approximant

As discussed in Section 3 and illustrated in Section 3.5.1, branch points in the parameter space that are close to the parameter path cause problems for the Padé approximation. If none of the poles of $[L/M]_{x_j}$ are close to a current parameter value on the path, we may be able to take a reasonably large step forward without getting into difficulties. However, since we take L and M to be small, we cannot expect the approximants $[L/M]_{x_j}$ to have already converged in a disk with radius the distance to the nearest singularity. Nor can we expect that the poles of $[L/M]_{x_j}$ are very good approximations of the actual singularities. Taking the distance D to the most nearby pole of $[L/M]_{x_j}$ as an estimate for the convergence radius is a very rough estimate in this case. However, we observe that D does give an estimate of the order of magnitude of the region in which $[L/M]_{x_j}$ is a satisfactory approximation. The conclusion is that we do not use D itself, but $\beta_2 D$ where $0 < \beta_2 < 1$ is a safety factor.

5.1.4 The candidate stepsizes Δt_1 and Δt_2

We now use the ingredients presented above to compute two candidate stepsizes Δt_1 and Δt_2 . For Δt_1 , we use the estimate η_{i,t^*} for the distance to the nearest path and the estimate $\|e_0\| |\Delta t|^k$ for the approximation error of the Padé approximant. The heuristic is that we want the approximation error to be only a small fraction of the estimated distance to the nearest path, so that the predicted point \tilde{z} is much closer to the path being tracked than to the nearest different path. That is, we solve $\|e_0\| |\Delta t_1|^k = \beta_1 \eta_{i,t^*}$ for Δt_1 , where $\beta_1 > 0$ is a small factor. Since the attraction bassins of Newton correction can behave in unexpected ways, it is best to take β_1 to be fairly small, for instance $\beta_1 = 0.005$. This gives

$$\Delta t_1 = \sqrt[k]{\beta_1 \eta_{i,t^*} \|e_0\|^{-1}}. \quad (17)$$

Both the estimates η_{i,t^*} and $\|e_0\| |\Delta t|^k$ are only accurate in case trouble is near (they are based on lowest order approximations). The case when $\|e_0\| \approx 0$ causes trouble in the formula for Δt_1 , but for too small values of $\|e_0\|$, we may set Δt_1 simply to one. If the resulting Δt_1 is large, the only thing this tells us is that we are not on a difficult point on the path with high probability. The second candidate stepsize, Δt_2 , will make sure we don't take a step that is too large in this situation. At the same time, Δt_2 will be small when singularities in the parameter space are near the current point on the path. Let D be the distance to the nearest pole out of all the poles of the $[L/M]_{x_j}, j = 1, \dots, n$. We set

$$\Delta t_2 = \beta_2 D \quad (18)$$

where $0 < \beta_2 < 1$ is a safety factor which should not change the order of magnitude, for instance $\beta_2 = 0.5$.

Example 3. As mentioned above, the estimate η_{i,t^*} for the distance to the nearest different path is only accurate when another path is actually near. If this is not the case, Δt_1 may be too large and we need Δt_2 to make sure the resulting stepsize is still safe. To see that it is not enough to take only Δt_2 into account, consider the homotopy

$$H(x, t) = (x - (t - (a + b\sqrt{-1}))^2)(x + (t - (a + b\sqrt{-1}))^2), \quad t \in [0, 1],$$

with $a, b \in \mathbb{R}$, $0 < a < 1$ and $|b|$ small. The paths corresponding to the two solutions are smooth and can be analytically continued in the entire complex plane: there are no singular points in $x_1(t), x_2(t)$. However, for $t = a + b\sqrt{-1}$ the two solutions coincide. By the assumptions on a and b , this value of t lies close to the parameter path $[0, 1]$. Intuitively, the singularity of the Jacobian $J_H = \partial H / \partial x$ is canceled by a zero of $\partial H / \partial t$: along the solution paths we have

$$\frac{dx}{dt} = \frac{-\frac{\partial H}{\partial t}}{\frac{\partial H}{\partial x}} = \frac{4(t - (a + b\sqrt{-1}))^3}{2x} = \frac{4(t - (a + b\sqrt{-1}))^3}{\pm 2(t - (a + b\sqrt{-1}))^2} = \pm 2(t - (a + b\sqrt{-1})).$$

For $t = a$, the solutions are $x_1 = -b^2, x_2 = b^2$, so for small b , the paths are very close to each other. The type (1,1) Padé approximant will have no poles (or will only have very large ones due to numerical artefacts), so taking only this criterion into account would allow for taking large steps. However, the estimate (12) at $t = a$ gives $|\Delta z| \approx 4b^2/2$, which is exactly the distance to the nearest different path. \triangle

5.2 Path tracking algorithm

We are now ready to present the path tracking algorithm. Since our contribution is in the predictor step (line 6 in Algorithm 1), we focus on this part. The predictor algorithm is Algorithm 3 below. It is straightforward to embed this predictor algorithm in the template Algorithm 1.

Algorithm 3 Predictor algorithm

```

1: procedure Predict( $H, z_{t^*}^{(i)}, t^*, L, M, \beta_1, \beta_2, t_{\text{EG}}$ )
2:  $\{x_1(t), \dots, x_n(t)\} \leftarrow$  series solution of  $H$  at  $t = t^*$  computed up to order  $L + M + 2$ 
   such that  $x(0) = z_{t^*}^{(i)}$ 
3:  $D \leftarrow \infty$ 
4: compute  $\eta_{i,t^*}$  as in Definition 5.1
5: for  $j = 1, \dots, n$  do
6:    $p_j, q_j \leftarrow \text{PadéApprox}(x_j(t), L, M)$ 
7:   compute  $e_{0,j}$  using (15)
8:    $D \leftarrow \min\{D, \min\{|z| \mid q_j(z) = 0\}\}$ 
9: end for
10:  $e_0 \leftarrow (e_{0,1}, \dots, e_{0,n})$ 
11:  $\Delta t_1 \leftarrow \sqrt[k]{\frac{\beta_1 \eta_{i,t^*}}{\|e_0\|}}$ 
12:  $\Delta t_2 \leftarrow \beta_2 D$ 
13:  $\Delta t \leftarrow \min\{\Delta t_1, \Delta t_2, t_{\text{EG}} - t^*\}$ 
14:  $\tilde{z} \leftarrow (p_1(\Delta t)/q_1(\Delta t), \dots, p_n(\Delta t)/q_n(\Delta t))$ 
15: return  $\tilde{z}, \Delta t$ 
16: end procedure

```

We briefly discuss some of the steps in Algorithm 3. In step 2, The algorithm of [10] is used. We included a description of the algorithm and a proof of convergence in Section 4. The point around which we compute the series is t^* , the current parameter value on the path. The parameter $w = L + M + 2$ is the number of coefficients needed to compute the Padé approximant of type (L, M) and the approximation error estimate. The starting value of the power series is the constant vector $x^{(0)} = z_{t^*}^{(i)}$, satisfying $H(z_{t^*}^{(i)}, t^*) = 0$ such that convergence of the algorithm in [10] is guaranteed. In step 6, the type (L, M) Padé approximant of the coordinate function $x_j(t)$ is computed using the algorithm of [25]. Algorithm 3 has some more input parameters than the predictor in the template algorithm. We will usually take M very small (and often 1), motivated by the conclusions of Section 3. The value of L is chosen, for instance, such that $L + M + 2$ is a power of 2 e.g. $L = 5, M = 1$, because of the quadratic convergence property of the power series algorithm proved in Proposition 4.2. Reasonable values for β_1, β_2 are $\beta_1 = 0.005, \beta_2 = 0.5$ as stated before. The parameter t_{EG} is the beginning of the endgame operating region as in Section 2.

5.3 Complexity analysis

To conclude this section, we analyze the cost of one predictor-corrector step of our adaptive stepsize algorithm as a function of the number of variables n . The total cost of the algorithm consists roughly out of two main parts: the cost of the numerical linear algebra and the evaluation/differentiation operations.

Lemma 5.2. *Consider a homotopy in n variables. Let $L + M + 1$ be $O(n)$. The cost of the linear algebra operations of Algorithm 3 is $O(n^4)$.*

Proof. The dominant linear algebra operations in Algorithm 3 are the following:

- line 2: solving a lower triangular block Toeplitz linear system,
- line 4: computing the SVD of the Hessian matrices \mathcal{H}_i ,
- line 6: computing the Padé approximant from the series coefficients,
- line 8: computing the roots of the denominators of the Padé approximants.

The lemma will follow from investigating the complexity of each of these computations.

Exploiting the block structure of the linearized representations of the power series, the cost of the linear algebra operations in one Newton step on a series truncated to degree ℓ requires $O(n^3) + O(\ell n^2)$ operations [10]. In our application, $\ell = L + M + 1$, which is $O(n)$. Counting on the quadratic convergence of Newton's method, we need $O(\log(n))$ steps, so the linear algebra cost to compute the power series is $O(\log(n)n^3)$, which is $O(n^4)$.

The cost of one SVD decomposition of an n -by- n matrix is $O(n^3)$, see e.g. [17, Section 5.4]. The bound (17) requires n SVD decompositions, so we obtain $O(n^4)$.

The power series are input to n Padé approximants of degrees L and M , bounded by $O(n)$, as solutions of linear systems of size $O(n)$. The total cost of computing the coefficients of the Padé approximants is bounded by $O(n^4)$.

The pole distance requires the computation of the roots of the denominators of the Padé approximants. The denominators have degree M and M is $O(n)$. Computing all eigenvalues of n companion matrices is $O(n^4)$ using classical eigenvalue algorithms, and $O(n^3)$ using a specialized algorithm, e.g. [2].

Thus the cost of all linear algebra operations is $O(n^4)$. □

Lemma 5.3. *The cost to differentiate and evaluate the n Hessians \mathcal{H}_k is $2n$ times the cost of computing the Jacobian matrix J_H .*

Proof. We apply a result from algorithmic differentiation, see [26] and in particular [14]. Let f be a function in n variables. If W_f is the cost to evaluate f and its gradient, then the cost of the evaluation of the Hessian matrix of f is $2nW_f$. The lemma follows by application of this result to all polynomials h_i in the homotopy H . □

Lemma 5.4. *Let W_N be the cost of evaluation and differentiation for applying Newton's method on $H(x, t)$ at $(z_{t^*}, t^*) \in X \times \mathbb{C}$. The cost of evaluation and differentiation for applying Newton's method on $H(x, t)$ at the series $x(t)$ truncated at degree $O(n)$ is $O(n \log(n))W_N$.*

Proof. If we evaluate a polynomial in a power series, then we have to perform as many multiplications of power series as there are multiplications in the evaluation of the polynomial at constant numbers. The cost overhead is therefore the cost to multiply two power series, denoted by $M(n)$ for power series truncated to degree n . According to [12], $M(n)$ is $O(n \log(n))$. □

The lemmas lead to the following result.

Theorem 5.5. *The cost overhead of the a priori adaptive step control algorithm (Algorithm 3) relative to the a posteriori adaptive step control algorithm for a homotopy in n variables is at most $O(n \log(n))$.*

Proof. Consider a predictor-corrector step in an a posteriori step control algorithm. The predictor is typically a fourth order extrapolator and runs in $O(n)$. The corrector applies a couple of Newton steps, which requires $O(n^3)$ linear algebra operations and with evaluation and differentiation cost W_N . According to Lemma 5.2, the cost overhead of the linear algebra operations is $O(n)$. By Lemma 5.3,

$O(n)$ is also the cost overhead for the computation of the Hessians. The $O(n \log(n))$ is provided by Lemma 5.4. \square

We comment on the “*at most $O(n \log(n))$* ” in Theorem 5.5.

1. *The cost of evaluation/differentiation relative to linear algebra.*

For very sparse polynomial systems, the cost of evaluation and differentiation could be independent of the degrees and as low as for example $O(n^2)$, or even $O(n)$. In that case, the evaluation and differentiation cost to compute the power series would be $O(n^3 \log(n))$, or even as low as $O(n^2 \log(n))$. In both cases, the cost of the linear algebra operations would dominate and the cost overhead drops to $O(n)$.

2. *The value of $\ell = L + M + 1$ versus n .*

Our analysis was based on the assumption that ℓ is $O(n)$. For many polynomial systems arising in applications, the number of variables $n \lesssim 10$. A typical value for ℓ is 7, as our default values for L and M are 5 and 1 respectively, so our assumption is valid.

For cases when $n \gg \ell$, the cost overhead of working with power series then becomes $O(\ell \log(\ell))$, and ℓ may even remain fixed to eight. In cases when $n \gg \ell$, the cost overhead drops again to $O(n)$ as the cost of linear algebra operations dominates.

The focus of our cost analysis was on one step of applying our a priori adaptive step control algorithm and not on the total cost of tracking one entire path. This cost depends on the number of steps required to track a path. We observe in experiments (see Section 6) that using our algorithm some paths can be tracked successfully by taking only very few steps, even for high degree problems.

6 Numerical experiments

In this section we show some numerical experiments to illustrate the effectiveness of the techniques proposed in this article. The proposed method is implemented in PHCpack (v2.4.72), available at <https://github.com/janverschelde/PHCpack>, and in Padé.jl, an implementation of our algorithm in Julia. In the experiments, our implementations are compared with the state of the art. We will use the following short notations for the different solvers in our experiments:

<code>brt_DP</code>	Bertini v1.6 using double precision arithmetic (MPTYPE = 0) [5],
<code>brt_AP</code>	Bertini v1.6 using adaptive precision (MPTYPE = 2) [4],
<code>HC.jl</code>	HomotopyContinuation.jl v1.1 [11],
<code>phc -p</code>	The <code>phc -p</code> command of PHCpack v2.4.72 [60],
<code>phc -u</code>	Our algorithm, used in PHCpack v2.4.72 via <code>phc -u</code> ,
<code>Padé.jl</code>	Our algorithm, implemented in Julia.

We use default double precision settings for all these solvers, except `brt_AP`, for which we use default adaptive precision settings. The experiments in all but the last subsection are performed on an 8 GB RAM machine with an intel Core i7-6820HQ CPU working at 2.70 GHz. We restrict all solvers to the use of only one core for all the experiments, unless stated otherwise. We will use $\Gamma : [0, 1] \mapsto \mathbb{C} : s \mapsto s$, which will be a smooth parameter path as defined in Section 2 by the constructions in the experiments. Therefore, the parameter s will not occur in this section and paths are of the form $\{(x(t), t), t \in [0, 1]\} \subset X \times [0, 1]$. In all experiments, we use $\beta_1 = 0.005, \beta_2 = 0.5$. To measure the quality of a numerical solution of a system of polynomial equations, we compute its residual as a measure for the relative backward error. We use the definition of [52, Section 7] to compute the residual.

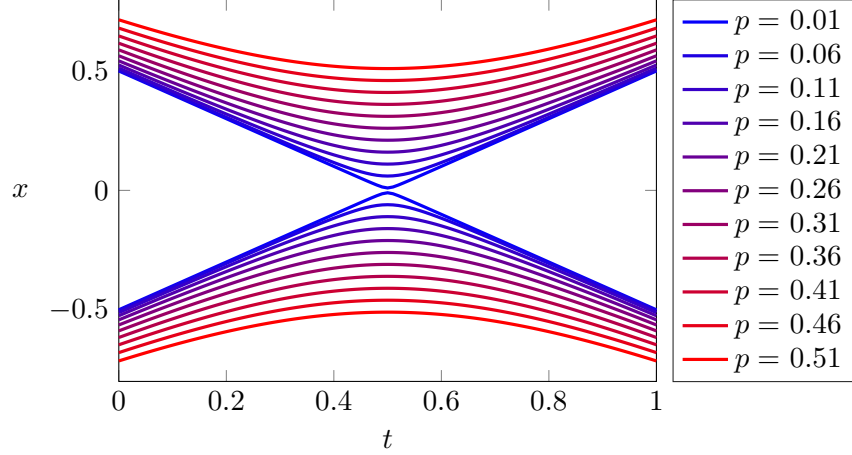


Figure 10: Family of hyperbolas from Subsection 6.1.

Solver \ k	1	2	3	4	5	6	7
brt_DP	✓	✓	✓	✗	✗	✗	✗
brt_AP	✓	✓	✓	✓	✗	✗	✗
HC.jl	✓	✗	✗	✗	✗	✗	✗
phc -p	✓	✗	✗	✗	✗	✗	✗
phc -u	✓	✓	✓	✓	✓	✓	✓

Table 1: Results of the experiment of Subsection 6.1 for $p = 10^{-k}$, $k = 1, \dots, 7$. A ‘✗’ indicates that path jumping happened.

6.1 A family of hyperbolas

Consider again the homotopy (1) from Example 1, which represents a family of hyperbolas parametrized by the real parameter p . Recall that the ramification locus is $S = \{1/2 + p\sqrt{-1}\}$. We will consider $p \neq 0$ here, such that $[0, 1]$ is a smooth parameter path. The smaller $|p|$, the closer the branch points move to the line segment $[0, 1]$. Figure 10 shows that as the value of $p > 0$ decreases, the two solution paths approach each other for parameter values $t^* \approx 0.5$ which causes danger for path jumping. This is confirmed by our experiments. Table 1 shows the results. We used $L = 5$, $M = 1$ in **phc -u**. The Julia implementation **HC.jl** checks whether the starting solutions are (coincidentally) solutions of the target system. For this reason, with this solver, we track for $t \in [0.1, 1]$.

6.2 Wilkinson polynomials

As a second experiment, consider the Wilkinson polynomial $W_d(x) = \prod_{i=1}^d (x - i)$ for $d \in \mathbb{N}_{>0}$. When $d > 10$, it is notoriously hard to compute the roots of these polynomials numerically when they are presented in the standard monomial basis. For Bertini and HomotopyContinuation.jl, we use the blackbox solvers to find the roots of the $W_d(x)$. In PHCpack, we use

$$H(x, t) = (x^d - 1)(1 - t) + \gamma W_d(x)t$$

with γ a random complex number³. The case $d = 12$ is illustrated in Figure 11. We use default settings for other solvers and $L = 5$, $M = 1$ in our algorithm to solve $W_d(x)$ for $d = 10, \dots, 19$. The results are reported in Table 2. The number e is the number of failures, i.e. d minus the number

³The other solvers use $\Gamma(s) = 1 - s$ by default. This is not important here.

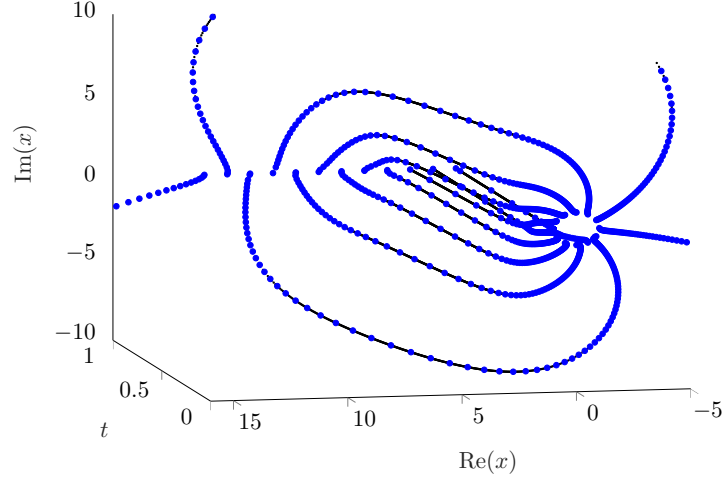


Figure 11: Solution paths for a random linear homotopy as in Subsection 6.2 connecting the 12th roots of unity to the roots of $W_{12}(x)$. The blue dots are the numerical approximations of points on the paths computed by our algorithm using $L = M = 1$.

d	phc -p		HC.j1		brt_DP		brt_AP		phc -u	
	e	T	e	T	e	T	e	T	e	T
10	5	8.0e-3	0	2.5e-3	0	4.5e-2	0	2.5e-2	0	4.0e-2
11	7	2.9e-2	0	3.6e-3	0	1.9e-1	0	1.4e+0	0	5.2e-2
12	9	3.4e-2	0	6.7e-3	0	1.5e-1	0	2.0e+0	0	6.9e-2
13	10	3.5e-2	0	4.1e-3	0	3.2e-1	0	2.8e+0	0	1.1e-1
14	11	2.4e-2	1	6.2e-3	0	4.8e-1	0	3.8e+0	0	1.0e-1
15	13	1.7e-2	1	9.0e-3	15	1.5e-2	15	1.6e-2	0	1.2e-1
16	15	2.1e-2	6	6.7e-3	16	1.6e-2	16	1.4e-2	0	1.7e-1
17	16	1.6e-2	10	3.2e-3	17	1.8e-2	17	1.3e-2	0	1.9e-1
18	18	6.0e-3	11	1.4e-2	18	1.8e-2	18	1.4e-2	0	2.4e-1
19	18	1.8e-2	13	7.0e-3	19	1.8e-2	19	1.4e-2	0	2.6e-1

Table 2: Results for the experiment of Subsection 6.2.

of distinct solutions (up to a certain tolerance) returned by each solver with residual $< 10^{-9}$, and T is the computation time in seconds. The column indexed by ‘#’ gives the minimum and maximum number of steps on a path for our solver. We conclude this section with a brief comparison with certified tracking algorithms. For $W_4(x)$, the algorithm⁴ proposed in [8] takes 6261.6 steps for the path starting at $z_0 = -1$ (this is averaged out over 5 experiments with random, rational γ). For $W_{15}(x)$ the certified tracking algorithm of [64] (which is specialized for the univariate case) takes on average 790 steps per path.

6.3 Generic polynomial systems

In this subsection, we consider random, square polynomial systems and solve them using the different homotopy continuation packages and the algorithm proposed in this paper. We now specify what ‘random’ means. Fix n and $d \in \mathbb{N} \setminus \{0\}$. A *generic polynomial system* of dimension n and degree d is given by $F : \mathbb{C}^n \rightarrow \mathbb{C}^n : x \mapsto (f_1(x), \dots, f_n(x))$ where

$$f_i(x) = \sum_{|q| \leq d} c_{i,q} x^q \in R = \mathbb{C}[x_1, \dots, x_n],$$

⁴We use a Macaulay2 implementation, available at <http://people.math.gatech.edu/~aleykin3/RobustCHT/> to perform these experiments.

n	d	phc -p		HC.jl		brt_DP		brt_AP		phc -u		
		e	T	e	T	e	T	e	T	e	T	# h
1	20	0	5.0e+0	0	1.7e-3	0	3.1e-2	0	7.5e-2	0	4.2e-2	6-16 0.09
	50	0	2.6e-2	0	6.3e-3	0	1.3e-1	0	2.3e+0	0	2.4e-1	5-27 0.07
	100	2	9.1e-2	0	1.1e-2	49	5.3e-1	0	1.2e+1	0	8.9e-1	4-27 0.13
	200	2	2.7e-1	0	3.2e-2	97	1.6e+0	1	4.5e+1	0	2.9e+0	5-25 0.13
	300	5	6.6e-1	×	×	221	2.8e+0	27	3.3e+2	0	8.3e+0	4-49 0.13
2	10	0	1.8e-1	0	1.5e-2	0	3.8e-1	0	2.4e+0	0	2.1e+0	8-37 0.10
	20	2	2.2e+0	0	8.9e-2	0	1.4e+1	0	1.2e+2	0	2.6e+1	8-55 0.13
	30	8	1.2e+1	0	3.3e-1	0	9.9e+1	0	2.0e+3	0	1.3e+2	8-68 0.13
	40	22	3.7e+2	0	9.1e-1	68	3.5e+2	0	7.8e+3	0	4.2e+2	6-57 0.15
	50	39	8.7e+2	0	2.3e+0	12	1.4e+3	0	3.4e+4	0	1.0e+3	7-57 0.14
3	5	0	3.5e-1	0	3.0e-2	0	7.0e-1	0	7.0e-1	0	4.8e+0	9-55 0.09
	9	1	8.5e+0	0	2.3e-1	0	2.1e+1	0	4.8e+1	0	9.8e+1	8-56 0.10
	13	4	6.8e+1	0	1.5e+0	0	2.3e+2	0	1.0e+3	0	8.3e+2	8-85 0.11

Table 3: Results for the experiment of Subsection 6.3.

with $q = (q_1, \dots, q_n) \in \mathbb{N}^n$, $|q| = q_1 + \dots + q_n$ and $c_{i,q}$ are complex numbers whose real and imaginary parts are drawn from a standard normal distribution. The *solutions* of F are the points in the fiber $F^{-1}(0) \subset \mathbb{C}^n$, and by Bézout's theorem, there are d^n such points. In order to find these solutions, we track the paths of the homotopy

$$H(x, t) = G(x)(1 - t) + \gamma F(x)t, \quad t \in [0, 1]$$

where γ is a random complex constant and $G : \mathbb{C}^n \rightarrow \mathbb{C}^n : x \mapsto (x_1^d - 1, \dots, x_n^d - 1)$ represents the *start system* with d^n known, regular solutions. Results are given in Table 3. In the table, n and d are as in the discussion above and e is the number of failures (i.e. d^n minus the number of successfully computed solutions, as in Subsection 6.2). For **phc -u**, the column indexed by ‘#’ gives the minimum and maximum number of steps on a path, and the column indexed by h gives the ratio of the number of steps for which $\Delta t = \Delta t_1$ is the first candidate stepsize. In this experiment, we took $L = 5, M = 1$ and we set the maximum stepsize to be 0.5. Note that even for this type of generic systems, the ‘difficulty’ of the paths (based on the number of steps needed) can vary strongly. The case $n = 1, d = 300$ is not supported by **HC.jl**, because only one byte is used to represent the degree. Note that **HC.jl** performs extremely well in all other cases in this experiment, both in terms of speed and robustness. The extra comparative experiment in the next subsection will show that, for difficult (non-generic) paths, our heuristic shows better results (this was also shown in Subsections 6.1 and 6.2).

6.4 Clustered solutions

Homotopies that cause danger for path jumping are such that for some parameter value t^* on the path, the map $H(x, t^*)$ is a polynomial system with some solutions that are clustered together. Motivated by this, we construct the following experiment. Let n_c be a parameter representing the number of solution clusters and let CS represent the ‘cluster size’. We consider the set of clusters $\{C_1, \dots, C_{n_c}\}$ where $C_i = \{z_{i,1}, \dots, z_{i,\text{CS}}\} \subset \mathbb{C}$ is a set of complex numbers that are ‘clustered’ in the following sense. Take $c_i = e^{\frac{i-1}{n_c} 2\pi\sqrt{-1}}$ and for a real parameter α , we define $z_{i,j} = c_i + \alpha u^{1/\text{CS}} e^{\frac{j-1}{\text{CS}} 2\pi\sqrt{-1}}$, where u is the unit roundoff ($\approx 10^{-16}$ in double precision arithmetic). Define the polynomial $E(x) = \prod_{i=1}^{n_c} (\prod_{j=1}^{\text{CS}} (x - z_{i,j}))$. The situation is illustrated in Figure 12 for $n_c = \text{CS} = 5, \alpha = 100$. For $\alpha = 1$, we know from classical perturbation theory of univariate polynomials that the roots of $E(x)$ look like the roots of a slightly perturbed version of a polynomial whose n_c roots are the cluster centers, which have multiplicity CS. We will use $\alpha \geq 10$, such that the roots of $E(x)$ are not ‘numerically singular’. Let $d = n_c \text{CS}$. Let $G(x) = x^d - 1$ and let $F(x)$ be a polynomial of degree d with random complex coefficients, with real and imaginary part drawn from a standard normal distribution. We consider the homotopy

$$H(x, t) = (1 - t)(1/2 - t)G(x) + \gamma_1 t(1 - t)E(x) + \gamma_2 t(1/2 - t)F(x), \quad t \in [0, 1]$$

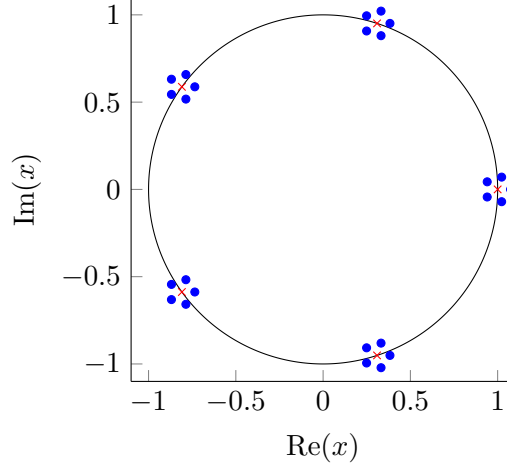


Figure 12: Roots (blue dots) and cluster centers (red crosses) of $E(x)$ constructed as in Subsection 6.4 with $n_c = \text{CS} = 5$, $\alpha = 100$.

α	Solver	CS				
		1	2	3	4	5
10	HC.jl	1.0	0.740	0.100	0.060	0.080
	Padé.jl	1.0	0.990	0.993	0.995	0.988
100	HC.jl	1.0	1.0	0.627	0.985	0.980
	Padé.jl	1.0	1.0	1.0	0.985	0.996
1000	HC.jl	1.0	1.0	1.0	1.0	1.0
	Padé.jl	1.0	1.0	0.987	1.0	1.0

Table 4: Results for $n_c = 5$.

α	Solver	CS				
		1	2	3	4	5
10	HC.jl	1.0	0.095	0.083	0.078	0.504
	Padé.jl	1.0	0.995	1.0	1.0	0.990
100	HC.jl	1.0	0.530	0.673	0.982	1.0
	Padé.jl	1.0	1.0	0.997	0.988	1.0
1000	HC.jl	1.0	0.995	0.990	1.0	0.310
	Padé.jl	1.0	0.995	0.997	1.0	0.992

Table 5: Results for $n_c = 10$.

where γ_1 and γ_2 are random complex constants. $G(x)$ represents the start system with starting solutions the d -th roots of unity. By tracking the homotopy H , the polynomial $G(x)$ is continuously transformed into the random polynomial $F(x)$, passing through the polynomial $(\gamma_1/4)E(x)$ (for $t^* = 1/2$) with clustered solutions. The *success rate* (SR) of a numerical path tracker for solving this problem is defined as follows. Let \hat{d} be the number of points among the solutions of $F(x)$ that coincide with a point returned by the path tracker up to a certain tolerance (e.g. 10^{-6}). We set $\text{SR} = \hat{d}/d$. For fixed α, n_c, CS and track 10 homotopies $H(x, t)$ constructed as above with different random γ_i using HC.jl and Padé.jl. We compute the average success rate for these 10 runs. Results are reported in Tables 4 and 5. For each problem, the best average success rate is highlighted in blue.

6.5 Benchmark Problems

Parallel computations were applied for the problems in this section. For two families of structured polynomial systems, our experiments show that no path failures and no path jumpings occur, even when the number of solution paths goes past one million.

6.5.1 Hardware and software

The program for the experiments is available in the MPI folder of PHCpack, available in its source code distribution on github, under the current name `mpi2padcon`. The code was executed on two 22-core 2.2 GHz Intel Xeon E5-2699 processors in a CentOS Linux workstation with 256 GB RAM. The number of processes for each run equals 44. The root node manages the distribution of the start solutions and the collection of the end paths. In a static work load assignment, the other 43 processes

each track the same number of paths.

6.5.2 The katsura- n systems

The **katsura** family of systems is named after the problem posed by Katsura [31], see [32] for a description of its relevance to applications. The **katsura- n** problem consists of n quadratic equations and one linear equation. The number of solutions equals 2^n , the product of the degrees of all polynomials in the system.

Table 6 summarizes the characteristics and wall clock times on **katsura- n** , for n ranging from 12 to 20. While the times with HOM4PS-2.0para [34] are much faster than in Table 6, Table 3 of [34] reports 2 and 4 curve jumpings respectively for **katsura-19** and **katsura-20**. In the runs with the MPI version for our code, no path failures and no path jumpings happened.

The good results we obtained required the use of homogeneous coordinates. When tracking the paths first in affine coordinates, we observed large values for the coordinates, which forced too small step sizes, which then resulted in path failures.

Although the defining equations are nice quadrics, the condition numbers of the solutions gradually increase as n grows. For example, for $n = 20$, the largest condition number of the Jacobian matrix was of the order 10^7 , observed for 66 solutions. Table 6 reports the number of real solutions in the column with header **#real** and the number of solutions with nonzero imaginary part under the header **#imag**. The progression of the wall clock times in Table 6 illustrates that our new path tracking algorithm

n	#sols	#real	#imag	wall clock time (seconds)	
12	4,096	582	3,514	7.925e+1	1m 19s
13	8,192	900	7,292	2.081e+2	3m 28s
14	16,384	1,606	14,778	5.065e+2	8m 27s
15	32,768	2,542	30,226	1.456e+3	24m 16s
16	65,536	4,440	61,096	4.156e+3	1h 9m 16s
17	131,072	7,116	123,956	1.001e+4	2h 46m 50s
18	262,144	12,458	249,686	2.308e+4	6h 24m 15s
19	524,288	20,210	504,078	5.696e+4	15h 49m 20s
20	1,048,576	35,206	1,013,370	1.317e+5	36h 34m 11s

Table 6: Wall clock time on 44 processes on the **katsura** problem, in a static workload balancing schedule with one manager node and 43 worker nodes. Only the workers track solution paths.

scales well for increasing dimensions, despite the $O(n^4)$ factor in its cost.

6.5.3 A model of a neural network

An interesting class of polynomial systems [43] was introduced to the computer algebra community by [21]. The n -dimensional system consists of n cubic equations and originated from a model of a neural network. A linear-product root bound provides a sharp root count. Although the permutation symmetry could be exploited, with a symmetric homotopy using the algorithms in [61], this did not happen for the computations summarized in Table 7. Homogeneous coordinates were also applied in the runs. The formulation of the polynomials in [43] depends on one parameter c , which was set to 1.1. The number of real solutions are reported in Table 7 in the column with header **#real** and the number of solutions with nonzero imaginary part are under the header **#imag**. Because every new equation is of degree three and the number of paths triples, the wall clock time increases more than in the previous benchmark. As before, no path failures and no path jumpings happened.

n	#sols	#real	#imag	wall clock time (seconds)	
10	59,029	21	59,008	3.478e+3	57m 58s
11	177,125	23	177,102	1.594e+4	4h 25m 37s
12	531,417	25	531,392	7.202e+4	20h 0m 17s
13	1,594,297	27	1,594,270	3.030e+5	84h 9m 58s

Table 7: Wall clock times on 44 processes on polynomial systems modeling a neural network, in a static workload balancing schedule with one manager node and 43 worker nodes. Only the worker nodes track solution paths.

7 Conclusion and Future Work

We have proposed an adaptive stepsize predictor algorithm for numerical path tracking in polynomial homotopy continuation. The resulting algorithm can be used to solve challenging problems successfully using only double precision arithmetic and is competitive with existing software. An implementation is available in PHCpack (available on github). It is expected that analogous techniques can be used to track paths that contain singular points for $t \in [0, 1)$, to compute monodromy groups and to design efficient new end games for dealing with singular endpoints and solutions at infinity. Another possible direction for future research is to investigate whether the methods of this paper can be made certifiable, for instance by bounding the factors β_1, β_2 . One could also choose the parameters L and M based on an analysis of the Padé table at several points on the path. Finally, the use of generalized Padé approximants could speed up the computations [23].

Acknowledgements

We would like to thank two anonymous referees for their useful suggestions and comments on an earlier version of this paper.

References

- [1] E. L. Allgower and K. Georg. *Introduction to Numerical Continuation Methods*, volume 45 of *Classics in Applied Mathematics*. SIAM, 2003.
- [2] J. L. Aurentz, T. Mach, R. Vandebril, and D. S. Watkins. Fast and backward stable computation of roots of polynomials. *SIAM Journal on Matrix Analysis and Applications*, 36(3):942–973, 2015.
- [3] G. A. Baker Jr and P. Graves-Morris. *Padé Approximants*, volume 59. Cambridge University Press, 1996.
- [4] D. Bates, J. Hauenstein, A. Sommese, and C. Wampler. Adaptive multiprecision path tracking. *SIAM J. Numer. Anal.*, 46(2):722–746, 2008.
- [5] D. J. Bates, J. D. Hauenstein, A. J. Sommese, and C. W. Wampler. *Numerically Solving Polynomial Systems with Bertini*, volume 25. SIAM, 2013.
- [6] A. Beardon. On the location of poles of Padé approximants. *Journal of Mathematical Analysis and Applications*, 21(3):469–474, 1968.
- [7] B. Beckermann and A. C. Matos. Algebraic properties of robust Padé approximants. *Journal of Approximation Theory*, 190:91–115, 2015.
- [8] C. Beltrán and A. Leykin. Robust certified numerical homotopy tracking. *Foundations of Computational Mathematics*, 13(2):253–295, 2013.
- [9] L. Bieberbach. *Analytische Fortsetzung*, volume 3 of *Ergebnisse der Mathematik und Ihrer Grenzgebiete*. Springer-Verlag, 1955.
- [10] N. Bliss and J. Verschelde. The method of Gauss–Newton to compute power series solutions of polynomial homotopies. *Linear Algebra and its Applications*, 542:569–588, 2018.
- [11] P. Breiding and S. Timme. HomotopyContinuation.jl: A package for homotopy continuation in julia. In *International Congress on Mathematical Software*, pages 458–465. Springer, 2018.

- [12] R. P. Brent and H. T. Kung. Fast algorithms for manipulating formal power series. *Journal of the ACM (JACM)*, 25(4):581–595, 1978.
- [13] P. Bürgisser and F. Cucker. *Condition: The geometry of numerical algorithms*, volume 349. Springer Science & Business Media, 2013.
- [14] B. Christianson. Automatic Hessians by reverse accumulation. *IMA Journal of Numerical Analysis*, 12(2):135–150, 1992.
- [15] D. A. Cox, J. Little, and D. O’Shea. *Ideals, Varieties, and Algorithms*, volume 3. Springer, 1992.
- [16] R. de Montessus. Sur les fractions continues algébriques. *Bulletin de la Société Mathématique de France*, 30:28–36, 1902.
- [17] J. W. Demmel. *Applied numerical linear algebra*, volume 56. Siam, 1997.
- [18] P. Dienes. *The Taylor series: an introduction to the theory of functions of a complex variable*. Dover New York, 1957.
- [19] D. Eisenbud. *Commutative Algebra: with a view toward algebraic geometry*, volume 150. Springer Science & Business Media, 2013.
- [20] E. Fabry. Sur les points singuliers d’une fonction donnée par son développement en série et l’impossibilité du prolongement analytique dans des cas très généraux. In *Annales scientifiques de l’École Normale Supérieure*, volume 13, pages 367–399. Elsevier, 1896.
- [21] K. Gatermann. Symbolic solution of polynomial equation systems with symmetry. In S. Watanabe and M. Nagata, editors, *Proceedings of ISSAC-90 (Tokyo, Japan, August 20–24, 1990)*, pages 112–119. ACM, 1990.
- [22] J.-J. Gervais and H. Sadiky. A continuation method based on a high order predictor and an adaptive steplength control. *ZAMM-Journal of Applied Mathematics and Mechanics/Zeitschrift für Angewandte Mathematik und Mechanik: Applied Mathematics and Mechanics*, 84(8):551–563, 2004.
- [23] A. A. Gončar. On the convergence of generalized Padé approximants of meromorphic functions. *Mathematics of the USSR-Sbornik*, 27(4):503, 1975.
- [24] A. A. Gončar. Poles of rows of the Padé table and meromorphic continuation of functions. *Matematicheskii Sbornik*, 157(4):590–613, 1981.
- [25] P. Gonnet, S. Güttel, and L. N. Trefethen. Robust Padé approximation via SVD. *SIAM review*, 55(1):101–117, 2013.
- [26] A. Griewank and A. Walther. *Evaluating derivatives: principles and techniques of algorithmic differentiation*, volume 105. Siam, 2008.
- [27] B. Huber and B. Sturmfels. A polyhedral method for solving sparse polynomial systems. *Math. Comp*, 64:1541–1555, 1995.
- [28] B. Huber and J. Verschelde. Polyhedral end games for polynomial continuation. *Numerical Algorithms*, 18(1):91–108, 1998.
- [29] O. Ibryaeva and V. Adukov. An algorithm for computing a Padé approximant with minimal degree denominator. *Journal of Computational and Applied Mathematics*, 237:529–541, 2013.
- [30] G. Jeronimo, G. Matera, P. Solernó, and A. Weissbein. Deformation techniques for sparse systems. *Found. Comput. Math.*, 9:1–50, 2009.
- [31] S. Katsura. Users posing problems to PoSSO. In the PoSSO Newsletter, no. 2, July 1994, edited by L. Gonzelez-Vega and T. Recio.
- [32] S. Katsura. Spin glass problem by the method of integral equation of the effective field. In M. Coutinho-Filho and S. Resende, editors, *New Trends in Magnetism*, pages 110–121. World Scientific, 1990.
- [33] R. B. Kearfott and Z. Xing. An interval step control for continuation methods. *SIAM Journal on Numerical Analysis*, 31(3):892–914, 1994.
- [34] T. Li and C. Tsai. HOM4PS-2.0para: Parallelization of HOM4PS-2.0 for solving polynomial systems. *Parallel Computing*, 35(4):226–238, 2009.
- [35] T.-Y. Li. Numerical solution of multivariate polynomial systems by homotopy continuation methods. *Acta Numerica*, 6:399–436, 1997.
- [36] J. D. Lipson. Newton’s method: a great algebraic algorithm. In *Proceedings of the third ACM symposium on Symbolic and algebraic computation*, pages 260–270. ACM, 1976.
- [37] W. D. Mac Millan. A method for determining the solutions of a system of analytic functions in the neighborhood of a branch point. *Mathematische Annalen*, 72(2):180–202, 1912.

- [38] J. Maurer. Puiseux expansion for space curves. *Manuscripta Mathematica*, 32(1-2):91–100, 1980.
- [39] A. Morgan. *Solving polynomial systems using continuation for engineering and scientific problems*, volume 57 of *Classics in Applied Mathematics*. SIAM, 2009.
- [40] A. P. Morgan, A. J. Sommese, and C. W. Wampler. Computing singular solutions to nonlinear analytic systems. *Numerische Mathematik*, 58(1):669–684, 1990.
- [41] A. P. Morgan, A. J. Sommese, and C. W. Wampler. A power series method for computing singular solutions to nonlinear analytic systems. *Numerische Mathematik*, 63(1):391–409, 1992.
- [42] Y. Nakatsukasa, O. Sète, and L. N. Trefethen. The AAA algorithm for rational approximation. *SIAM Journal on Scientific Computing*, 40(3):A1494–A1522, 2018.
- [43] V. W. Noonburg. A neural network modeled by an adaptive Lotka-Volterra system. *SIAM J. Appl. Math.*, 49(6):1779–1792, 1989.
- [44] K. Piret and J. Verschelde. Sweeping algebraic curves for singular solutions. *Journal of Computational and Applied Mathematics*, 234(4):1228–1237, 2010.
- [45] H. Schwetlick and J. Cleve. Higher order predictors and adaptive steplength control in path following algorithms. *SIAM Journal on Numerical Analysis*, 24(6):1382–1393, 1987.
- [46] A. J. Sommese, J. Verschelde, and C. W. Wampler. Numerical decomposition of the solution sets of polynomial systems into irreducible components. *SIAM Journal on Numerical Analysis*, 38(6):2022–2046, 2001.
- [47] A. J. Sommese, J. Verschelde, and C. W. Wampler. Introduction to numerical algebraic geometry. In *Solving polynomial equations*, pages 301–337. Springer, 2005.
- [48] A. J. Sommese and C. W. Wampler. *The Numerical Solution of Systems of Polynomials Arising in Engineering Science*. World Scientific Publishing Co. Pte. Ltd., 2005.
- [49] H. Stahl. The convergence of Padé approximants to functions with branch points. *Journal of Approximation Theory*, 91(2):139–204, 1997.
- [50] S. P. Suetin. On an inverse problem for the m -th row of the Padé table. *Mathematics of the USSR-Sbornik*, 52(1):231, 1985.
- [51] S. P. Suetin. Padé approximants and efficient analytic continuation of a power series. *Russian Mathematical Surveys*, pages 43–141, 2002.
- [52] S. Telen and M. Van Barel. A stabilized normal form algorithm for generic systems of polynomial equations. *Journal of Computational and Applied Mathematics*, 342:119–132, 2018.
- [53] S. Timme. Adaptive step size control for polynomial homotopy continuation methods. *arXiv preprint arXiv:1902.02968*, 2019.
- [54] L. N. Trefethen. *Approximation theory and approximation practice*, volume 164. Siam, 2019.
- [55] L. N. Trefethen. Quantifying the ill-conditioning of analytic continuation. *SIAM J. Numer. Anal.*, 2019.
- [56] A. Trias. The holomorphic embedding load flow method. In *2012 IEEE Power and Energy Society General Meeting*, pages 1–8. IEEE, 2012.
- [57] A. Trias and J. L. Martin. The holomorphic embedding loadflow method for DC power systems and nonlinear DC circuits. *IEEE Transactions on Circuits and Systems*, 63(2):322–333, 2016.
- [58] J. van der Hoeven. Reliable homotopy continuation. Technical report, LIX, Ecole polytechnique, 2015.
- [59] V. V. Vasilov, V. A. Prokhorov, and S. P. Suetin. The poles of the m -th row of the Padé table and the singular points of a function. *Mathematics of the USSR-Sbornik*, 50(2):457, 1985.
- [60] J. Verschelde. Algorithm 795: PHCpack: A general-purpose solver for polynomial systems by homotopy continuation. *ACM Transactions on Mathematical Software (TOMS)*, 25(2):251–276, 1999.
- [61] J. Verschelde and R. Cools. Symmetric homotopy construction. *J. Comput. Appl. Math.*, 50:575–592, 1994.
- [62] J. Verschelde, P. Verlinden, and R. Cools. Homotopies exploiting Newton polytopes for solving sparse polynomial systems. *SIAM Journal on Numerical Analysis*, 31(3):915–930, 1994.
- [63] D. Wu and B. Wang. A holomorphic embedding based continuation method for identifying multiple power flow solutions. <https://arxiv.org/abs/1905.01602v1>.
- [64] J. Xu, M. Burr, and C. Yap. An approach for certifying homotopy continuation paths: Univariate case. In *Proceedings of the 2018 ACM International Symposium on Symbolic and Algebraic Computation, ISSAC ’18*, pages 399–406, New York, NY, USA, 2018. ACM.